Mullard Technical Communications

OCTOBER 1972
Volume 12 Number 116

Contents

- 170 Microstrip transmission lines: impedance matching, coupling and filtering
  - 170 Tapered transmission lines for impedance matching sections
  - 177 Microstrip directional couplers
  - 188 Interdigital filters and experimental microstrip filter design at 470 MHz
  - 193 A microstrip bandpass filter for 0·7 to 1·4GHz
- 197 A new method of colour purity adjustment

Mullard Limited Mullard House Torrington Place London WC1E 7HD

Mullard Technical Communications

VOLUME 12 NUMBER 116 October 1972

Microstrip transmission lines: impedance matching, coupling and filtering *M. Michaelides* 170

Tapered transmission lines for impedance matching sections 170

Microstrip directional couplers 177

Interdigital filters and experimental microstrip filter design at 470MHz 188

A microstrip bandpass filter for 0·7 to 1·4GHz 193

A new method of colour purity adjustment *J.Gerritsen* 197

This journal records developments in the application of electronics in science, industry, and the home. It contains information on the properties and performance of solid-state devices, valves and tubes, and associated components and assemblies. The practical circuits given are designed to provide the best working conditions and performance for the devices used. The design principles may be used (so far as device ratings allow) for adaptation to meet particular requirements. Current data should be consulted before any circuit is considered for production. Mullard Limited can normally supply only those devices or assemblies listed in the Company's current catalogues. Availability in quantity should be confirmed.

All information is published in good faith, but because of the wide variety of situations in which this information may be used, we cannot accept any responsibility for loss or damage resulting from unsatisfactory performance. Publication of this information does not imply any authority or licence for the utilisation of any patented feature.

Four issues are published each year and issued free of charge to equipment designers, research organisations, laboratories, libraries, educational establishments, and consultants. Requests for addition to the mailing list must be made on the official stationery of the establishment concerned.

Technical enquiries should be addressed to the Editor. Abstracts or references should mention both source and authors. Requests for republication or translation should be made to the Editor in writing.

'Mullard' is the trade mark of Mullard Limited and is registered in most of the principal countries of the world.

Editor: E. G. Evans
Central Technical Services. Telephone: 01-648 3471, Telex: 22194

Mullard Limited, Mullard House, Torrington Place, London, WC1E 7HD
Telephone: 01-580 6633 Telex: 264341

©Mullard Limited, 1972

Made and Printed in England by
WIGHTMAN AND COMPANY LIMITED, 1/3 BRIXTON ROAD, LONDON SW9 6DS

Microstrip transmission lines: impedance matching, coupling and filtering

M. MICHAELIDES
Mullard Central Application Laboratory

UDC 621.372.821:621.372.852.6
621.372.832.43
621.372.852.1

GENERAL INTRODUCTION

Microstrip transmission lines, constructed from narrow copper-cladding strips on a dielectric base, are robust, compact, and directly compatible with printed wiring board techniques. Such lines offer advantages in v.h.f., u.h.f. and microwave equipment.

The present article discusses the theory and construction of microstrip impedance matching sections, microstrip directional couplers, microstrip interdigital filters and microstrip bandpass filters. Computer programs or constructional details are provided.

This initial work was performed mostly at u.h.f. but can be applied to other frequency ranges: the frequencies chosen in each case, for the present work, are related to the operating frequency band of the u.h.f. amplifiers BGY22 and BGY23. These are small solid-state modules: the BGY22 delivers 2·5W output for 0·05W input, and the BGY23 delivers 7W output for 2·5W input, and so the two devices can be used in series. Both operate from 13·8V.

Tapered transmission lines for impedance matching sections

The effect of tapered transmission lines on reducing the mismatch between two lossless transmission lines is examined both theoretically and experimentally in this article.

A number of tapered lines, coaxial and microstrip, were designed with the aid of a computer. The lines were half wavelength long at 470MHz and were designed to match 75Ω to 50Ω. The computer program is provided.

The performance of the lines was measured over the frequency band of 200MHz to 1000MHz. It was found that, in general, the lines offered an improvement in the reflection coefficient. The best improvement was obtained from the microstrip exponential taper line.

INTRODUCTION

The mismatch between two lossless transmission lines of different characteristic impedance can be reduced by introducing either a taper of varying impedance or a series of quarter wavelength transformer sections. This article examines briefly the various types of tapers, and describes results obtained from a coaxial and three microstrip experimental tapered lines.

The lines were designed to be half wavelength long at 470MHz and match 50Ω line to 75Ω line. This frequency is within the operating frequency band of the amplifiers BGY22 and BGY23.

OUTLINE OF THE THEORY

The mismatch caused by an impedance step in a transmission line will produce a v.s.w.r., s, of

$$s = \frac{Z_T}{Z_0} \qquad \ldots(1)$$

where Z_0 is the characteristic impedance of the line and Z_T the terminating impedance. By definition the reflection coefficient ρ_0 is given by

$$\rho_0 = \frac{Z_T - Z_0}{Z_T + Z_0}. \qquad \ldots(2)$$

This can be expressed as

$$\rho_0 = \tfrac{1}{2}\log_e \frac{Z_T}{Z_0}. \qquad \ldots(3)$$

This gives a value within 4% for $\frac{Z_T}{Z_0} < 2$.

By introducing a section of tapered transmission line between the two impedances Z_0 and Z_T a variation of the reflection coefficient with wavelength can be obtained which is either smooth or consists of a major lobe followed by a series of minor lobes.

The shape of the curve depends on the profile of the taper chosen (Ref. 1). The exponential taper (Refs. 2 and 3) has a response characterised by a major lobe followed by a series of minor lobes, while the hyperbolic taper (Ref. 4) and the parabolic taper (Ref. 5) each have a response which gives a reflection coefficient gradually diminishing with frequency.

Fig. 1 gives the continuous taper notation between two lines of different characteristic impedances Z_0 and Z_T. $Z_{(x)}$ represents the characteristic impedance at a point situated at distance x from the beginning of the taper. For an exponential taper $Z_{(x)}$ is given as

$$Z_{(x)} = Z_0 \exp\left[\left(\frac{x}{\ell}\right)\log_e\left(\frac{Z_T}{Z_0}\right)\right]. \qquad \ldots(4)$$

Hence for $x = 0$

$$Z_{(x)}\big|_{x=0} = Z_0 \exp\left[(0)\times\log_e\frac{Z_T}{Z_0}\right] = Z_0, \qquad \ldots(5)$$

and for $x = \ell$

$$Z_{(x)}\big|_{x=\ell} = Z_0 \exp\left[(1)\times\log_e\left(\frac{Z_T}{Z_0}\right)\right] = Z_0\times\frac{Z_T}{Z_0} = Z_T. \qquad \ldots(6)$$

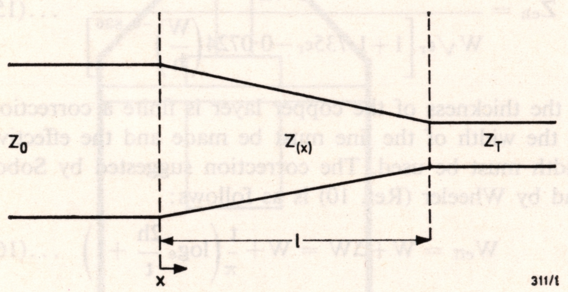

Fig. 1—Continuous taper notation

It can be seen that the taper matches at the two ends to the appropriate impedances.

COMPUTER PROGRAM

Computer program for calculating tapered transmission line profile

The magnitude of the reflection coefficient is given by

$$|\rho| = \frac{\sin\beta\ell}{\beta\ell}\,\tfrac{1}{2}\log_e\frac{Z_T}{Z_0}, \qquad \ldots(7)$$

where

$$\beta = \frac{2\pi}{\lambda_g}$$

where λ_g is the guide wavelength.
Using Eq. 3 we get

$$\left|\frac{\rho}{\rho_0}\right| = \frac{\sin\beta\ell}{\beta\ell}. \qquad \ldots(8)$$

The impedance profile of a hyperbolic taper is given by

$$Z_{(x)} = \frac{Z_T + Z_0}{2} + \frac{Z_T - Z_0}{2}\tanh a\left(\frac{x}{\ell} - 0{\cdot}5\right). \qquad \ldots(9)$$

The parabolic taper is given by the following equation

$$Z_{(x)} = Z_0 + 3(Z_T - Z_0)\left(\frac{x}{\ell}\right)^2 - 2(Z_T - Z_0)\left(\frac{x}{\ell}\right)^3. \qquad \ldots(10)$$

Fig. 2 gives the absolute value of the normalised reflection coefficient $|\rho/\rho_0|$ for the exponential, hyperbolic and parabolic tapers. The exponential curve is independent of the values of Z_0 and Z_T. It can be seen that there is a major lobe starting at unity falling to zero at $\ell/\lambda_g = 0{\cdot}5$. This is followed by a series of minor lobes, the first having a maximum value of 0·212 occurring at $\ell/\lambda_g = 0{\cdot}75$.

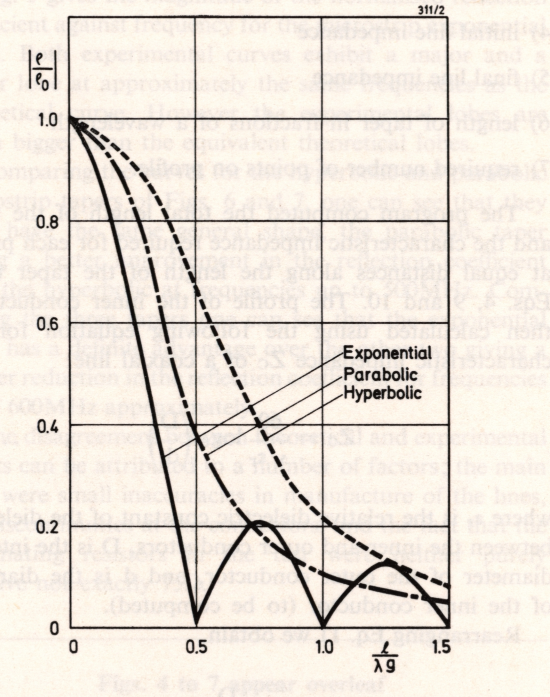

Fig. 2—Normalised reflection coefficient of various tapers

The curve of the hyperbolic taper is plotted for a = 6, $Z_0 = 50\Omega$ and $Z_T = 150\Omega$ and similarly the parabolic curve is plotted for $Z_0 = 50\Omega$ and $Z_T = 150\Omega$.

Other profiles have also been investigated. These include the 'Gaussian' taper (Ref. 6) the 'Willis-Sinha' optimum taper (Ref. 7) and the 'Dolph-Chebychev' optimum taper (Ref. 8).

COMPUTATION OF COAXIAL AND MICROSTRIP TAPERS

A computer program was developed to compute the profiles of either coaxial tapered lines or microstrip tapered lines, given the two impedances, frequency of operation, and the coaxial line or microstrip board information. The program computed the exponential, hyperbolic and parabolic tapered profiles. The program was writen in FORTRAN IV and takes 3 to 4 seconds to run on an IBM360. The program appears on page 175.

Coaxial tapers

The required input data is the following:

1) internal diameter of the outer conductor in centimetres (assumed constant)

2) relative dielectric constant for the dielectric between inner and outer conductors (= 1 for air line)

3) frequency of operation in Hz

4) initial line impedance

5) final line impedance

6) length of taper in fractions of a wavelength

7) required number of points on profile.

The program computed the total length of the taper and the characteristic impedance required for each profile at equal distances along the length of the taper using Eqs. 4, 9 and 10. The profile of the inner conductor is then calculated using the following equation for the characteristic impedance Z_C of a coaxial line:

$$Z_C = \frac{60}{\sqrt{\varepsilon_r}} \log_e \left(\frac{D}{d}\right) \qquad \ldots(11)$$

where ε_r is the relative dielectric constant of the dielectric between the inner and outer conductors, D is the internal diameter of the outer conductor, and d is the diameter of the inner conductor (to be computed).

Rearranging Eq. 11 we obtain,

$$d = \frac{D}{\exp\left(\frac{Z_C}{60}.\sqrt{\varepsilon_r}\right)} \qquad \ldots(12)$$

Microstrip tapers

The required input data is the following:

1) thickness of dielectric in centimetres

2) relative dielectric constant of dielectric board

3) thickness of copper layer in centimetres

4) frequency of operation in Hz

5) initial line impedance

6) final line impedance

7) length of taper in fractions of a wavelength

8) required number of points on profile.

The wavelength in microstrip is dependent on the dielectric constant of the substrate and, to a small extent, on the width of the microstrip line. Since the width of the line is varying along the taper, it was decided to use the line width corresponding to the geometric mean of the two end impedances Z_0 and Z_T to compute the required change of the wavelength. The equation for λ_g (the microstrip wavelength) as a function of λ_{TEM} (the TEM wavelength in the same dielectric medium) is given by Sobol (Ref. 9) as follows:

for $\frac{W}{h} > 0{\cdot}6$

$$\lambda_g/\lambda_{TEM} = \left[\frac{\varepsilon_r}{1+0{\cdot}63(\varepsilon_r-1)\left(\frac{W}{h}\right)^{0{\cdot}1255}}\right]^{\frac{1}{2}} \qquad \ldots(13)$$

and for $\frac{W}{h} < 0{\cdot}6$

$$\lambda_g/\lambda_{TEM} = \left[\frac{\varepsilon_r}{1+0{\cdot}6(\varepsilon_r-1)\left(\frac{W}{h}\right)^{0{\cdot}0297}}\right]^{\frac{1}{2}} \qquad \ldots(14)$$

where ε_r is the relative dielectric constant of the microstrip substrate, W the width of the microstrip line and h the substrate thickness.

The width of the microstrip line required for a given characteristic impedance can be computed from the following equation, as given by Sobol (Ref. 9):

$$Z_{ch} = \frac{377h}{W\sqrt{\varepsilon_r}\left[1+1{\cdot}735\varepsilon_r-0{\cdot}0724\left(\frac{W}{h}\right)^{-0.836}\right]} \qquad \ldots(15)$$

If the thickness of the copper layer is finite a correction to the width of the line must be made and the effective width must be used. The correction suggested by Sobol and by Wheeler (Ref. 10) is as follows:

$$W_{eff} = W+\Delta W = W+\frac{t}{\pi}\left(\log_e \frac{2h}{t}+1\right) \qquad \ldots(16)$$

where t is the thickness of the copper layer.

The width of the line corresponding to a certain characteristic impedance is then computed using an iteration process for each required point on the tapers. The characteristic impedance corresponding to each computed width is within 1% of the required value.

CONSTRUCTION OF THE TAPERS

The following four tapers were designed and built:

1) *An exponential coaxial line taper from 50Ω to 75Ω, λ/2 long at 470MHz.* The outer conductor has an internal diameter of 7·9mm kept constant along the length of the taper. The inner conductor has a diameter varying from 3·433mm at the 50Ω end to 2·263mm at the 75Ω end. Because of the difficulty of making a tapered conductor it was decided to vary the diameter in 20 steps at equal distances along the length. The 50Ω end of the line was terminated to a 50Ω male N-type connector whilst the 75Ω end was terminated to a 75Ω male BNC type connector. The centre conductor was supported in the middle by a thin p.t.f.e. ring.

2) *An exponential microstrip taper from 50Ω to 75Ω, λ/2 long at 470MHz.*

3) *A hyperbolic microstrip taper from 50Ω to 75Ω, λ/2 long at 470MHz.*

4) *A parabolic microstrip taper from 50Ω to 75Ω, λ/2 long at 470MHz.*

All microstrip tapers were built on Permaflon [relative dielectric constant = 2·74, thickness of substrate = 1·5875mm ($\frac{1}{16}$in), thickness of copper layer = 0·0762mm (0·003in, 2oz. copper]. The connections to the ends of the lines were made through General-Radio connectors, connected through the microstrip board as in Fig. 3.

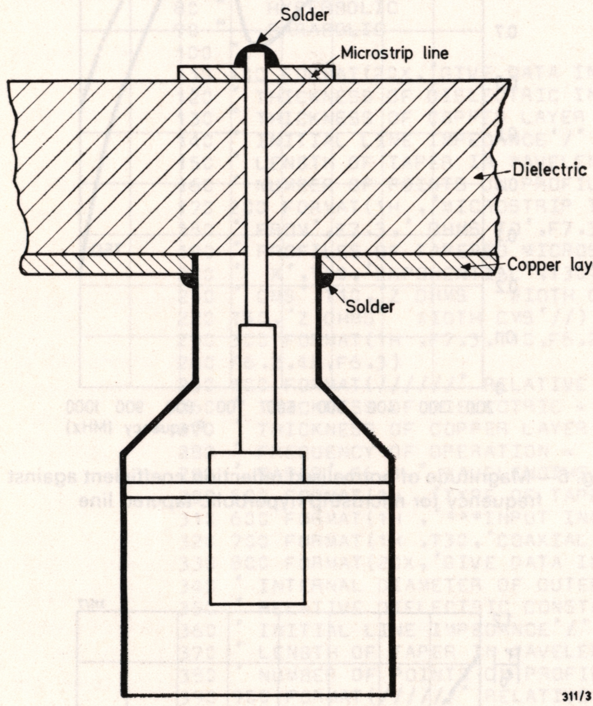

Fig. 3—Through-the-board connection to microstrip lines

EXPERIMENTAL RESULTS

The properties of the tapered lines were measured on the Hewlett-Packard Microwave Network Analyser. The two ends of each line were examined separately by comparing them with a standard 50Ω line on the Microwave Network Analyser and by calibrating with a short circuit. First the 75Ω end was measured by connecting it to a standard 50Ω input on the analyser which had been previously calibrated with a short circuit. (The 50Ω end of the taper being connected to the second 50Ω input.) The 50Ω end was then measured by connecting it to the calibrated 50Ω input on the analyser and terminating the 75Ω end with a 75Ω carbon resistor.

The normalised reflection coefficient was then calculated for both ends of the tapered lines and plotted in Figs. 4 to 7 on page 174.

Fig. 4 gives the magnitude of the normalised reflection coefficient against frequency for the coaxial exponential taper line, for the 75Ω end and the 50Ω end. The theoretical curve is also given.

The curve for the 50Ω end agrees reasonably well with the theoretical curve initially: it has a major lobe followed by a minor lobe. The agreement is reasonable to 800MHz at which point the curves start to rise dramatically whilst the theoretical curve continues to fall.

The main lobe of the 75Ω curve agrees well with the theoretical curve both in shape and size. However the experimental model exhibited no minor lobes and, in fact, it was found to rise continuously after the major lobe.

Fig. 5 gives the magnitude of the normalised reflection coefficient against frequency for the microstrip exponential taper. Both experimental curves exhibit a major and a minor lobe at approximately the same frequencies as the theoretical curve. However the experimental lobes are much bigger than the equivalent theoretical lobes.

Comparing the curves for the hyperbolic and parabolic microstrip tapers of Figs. 6 and 7, one can see that they both have the same general shape, the parabolic taper giving a better improvement in the reflection coefficient than the hyperbolic at frequencies up to 500MHz. Comparing the three tapers one can see that the exponential taper has a definite advantage over the other two giving a greater reduction in the reflection coefficient for frequencies up to 600MHz approximately.

The disagreement between theoretical and experimental results can be attributed to a number of factors; the main ones were small inaccuracies in manufacture of the lines, the discontinuities at the connectors, and the fact that the terminating resistors in the test were neither purely resistive nor exactly 75Ω.

Figs. 4 to 7 appear overleaf on page 174

The computer program appears on page 175

REFERENCES

1. Hall, A. H., 'Impedance Matching by Tapered or Stepped Transmission Lines', **Microwave Journal,** March 1966, pp. 109 to 114.
2. Burrows, C. R., 'The Exponential Transmission Line', **B.S.T.J.,** Vol. 17, October 1938, pp. 555 to 573.
3. Wheeler, H. A., 'Transmission Lines with Exponential Tapers', **Proc. IRE,** Vol. 27, January 1939, pp. 65 to 71.
4. Scott, H. J., 'The Hyperbolic Transmission Line as a Matching Section', **Proc. IRE,** Vol. 41, November 1953, pp. 1654 to 1657.
5. Young, R. F. H., 'Parabolic Transmission Line', Letter to **Proc. IRE,** Vol. 43, August 1955, pp. 1010.
6. Collin, R. E., 'The Optimum Tapered Transmission Line Matching Section'. **Proc. IRE,** Vol. 44, April 1956, pp. 539 to 548. Correction. Vol. 44, December 1956, p. 1753.
7. Willis, J., Sinha, N. K., 'Non-uniform Transmission Lines as Impedance Transformers'. **Proc. IEE,** Vol. 103B, March 1956, pp. 166 to 172. Also letter to **Proc. IRE,** Vol. 43, December 1955, p. 1975.
8. Klopfenstein, R. W., 'A Transmission Line Taper of Improved Design'. **Proc. IRE,** Vol. 44, January 1956, pp. 31 to 35.
9. Sobol, H., 'Extending I.C. Technology to Microwave Equipment'. **Electronics,** Vol. 40, pp. 112 to 124, March 20, 1967.
10. Wheeler, H. A., 'Transmission Line Properties of Parallel Strips Separated by a Dielectric Sheet'. **I.E.E.E. Transactions on Microwave Theory and Techniques,** MTT-13, March 1965, pp. 172 to 185.

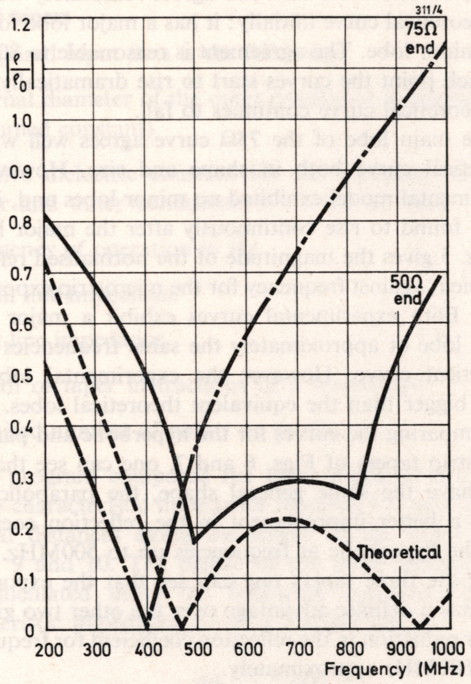

Fig. 4—Magnitude of normalised reflection coefficient against frequency for coaxial exponential tapered line

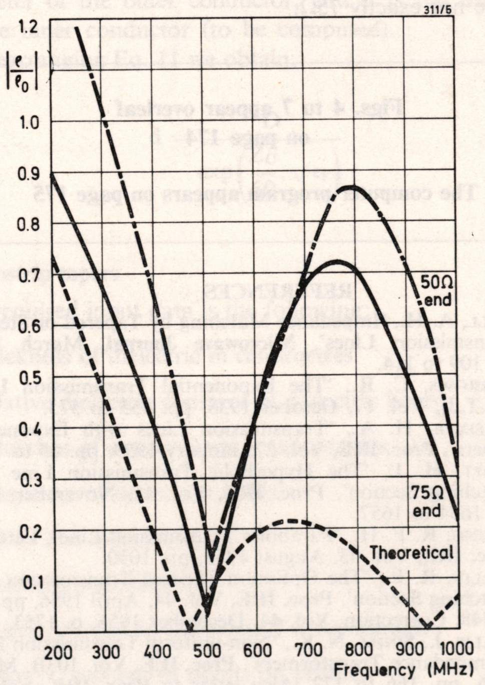

Fig. 5—Magnitude of normalised reflection coefficient against frequency for microstrip exponential tapered line

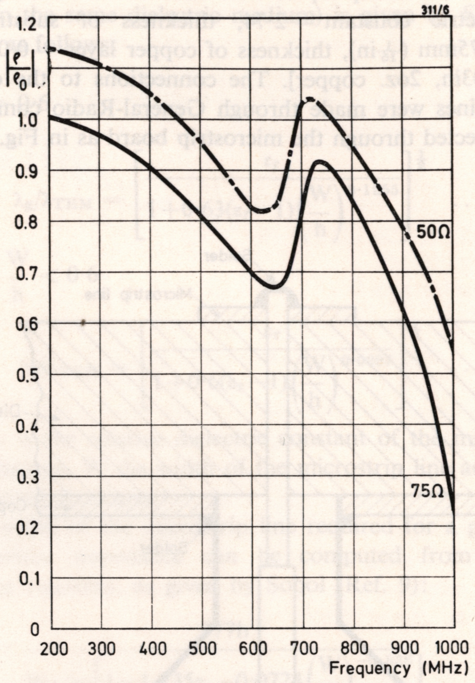

Fig. 6—Magnitude of normalised reflection coefficient against frequency for microstrip hyperbolic tapered line

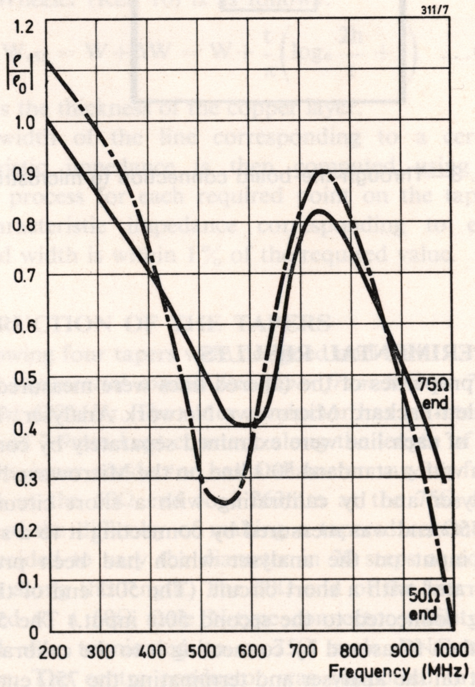

Fig. 7—Magnitude of normalised reflection coefficient against frequency for microstrip parabolic tapered line

Computer Program for Calculating Profiles of Tapered Microstrip and Coaxial Matching Sections

```
10 "    THIS PROGRAM COMPUTES THE PROFILES OF
20 "   TAPERED MICROSTRIP AND COAXIAL LINES
30 "   USED AS IMPEDANCE MATCHING SECTIONS.
40 "
50 "    THE PROFILES EXAMINED ARE:
60 "
70 "   EXPONENTIAL
80 "   HYPERBOLIC
90 "   PARABOLIC
100 "
110 100 FORMAT(20X,'GIVE DATA IN THE FOLLOWING ORDER:'//%
120  ' THICKNESS OF DIELECTRIC IN CMS'/' RELATIVE DIELECTRIC CONSTANT'/%
130  ' THICKNESS OF COPPER LAYER IN CMS'/' FREQUENCY IN HZ'/%
140  ' INITIAL LINE IMPEDANCE'/' FINAL LINE IMPEDANCE'/%
150  ' LENGTH OF TAPER IN WAVELENGTHS'/%
160  ' NUMBER OF POINTS ON PROFILE'////)
170 200 FORMAT(1H ,'MICROSTRIP TAPERS',F6.3,' WAVELENGTHS LONG'/%
180  ' FROM',F7.3,' OHMS TO',F7.3,' OHMS'//%
190  ' PROFILES OF TAPERED MICROSTRIP LINES'////%
200  ' X',T10,'EXPONENTIAL',T30,'HYPERBOLIC',T50,'PARABOLIC'/%
210  ' CMS',T10,'Z OHMS   WIDTH CMS',T30,'Z OHMS   WIDTH CMS',%
220 T50,'Z OHMS   WIDTH CMS'//)
230 300 FORMAT(1H ,F7.3,T10,F6.2,4X,F6.3,T30,F6.2,4X,F6.3,T50,%
240 F6.2,4X,F6.3)
250 400 FORMAT(//////' RELATIVE DIELECTRIC CONSTANT = ',F6.3/%
260  ' THICKNESS OF DIELECTRIC = ',F8.5,' CMS'/%
270  ' THICKNESS OF COPPER LAYER =  ',F8.5,' CMS'/%
280  ' FREQUENCY OF OPERATION = ',E10.3,' HZ'/%
290  ' TAPER',F6.3,' WAVELENGTHS LONG = ',F7.3,' CMS'//////)
300 500 FORMAT(1H ,'TYPE OF TAPER REQUIRED ? (COAXIAL=1,MICROSTRIP=2)')
310 600 FORMAT(1H ,'***INPUT INCORRECT. PLEASE RETYPE IT***')
320 700 FORMAT(1H ,T30,'COAXIAL TAPER'/T30,'-------------'//)
330 800 FORMAT(20X,'GIVE DATA IN THE FOLLOWING ORDER:'//%
340  ' INTERNAL DIAMETER OF OUTER CONDUCTOR IN CMS'/%
350  ' RELATIVE DIELECTRIC CONSTANT'/' FREQUENCY IN HZ'/%
360  ' INITIAL LINE IMPEDANCE'/' FINAL LINE IMPEDANCE'/%
370  ' LENGTH OF TAPER IN WAVELENGTHS'/%
380  ' NUMBER OF POINTS ON PROFILE'////)
390 900 FORMAT(//////' RELATIVE DIELECTRIC CONSTANT = ',F6.3/%
400  ' INTERNAL DIAMETER OF OUTER CONDUCTOR = ',F9.5,' CMS'/%
410  ' FREQUENCY OF OPERATION = ',E10.3,' HZ'/%
420  ' TAPER',F6.3,' WAVELENGTHS LONG = ',F7.3,' CMS'//////)
430 1000 FORMAT(1H ,'COAXIAL TAPERS',F6.3,' WAVELENGTHS LONG'/%
440  ' FROM',F7.3,' OHMS TO',F7.3,' OHMS'//%
450  ' PROFILES OF TAPERED CENTRE CONDUCTOR'////%
460  ' X',T10,'EXPONENTIAL'T30,'HYPERBOLIC',T50,'PARABOLIC'/%
470  ' CMS',T10,'Z OHMS   DIA. CMS'T30,'Z OHMS   DIA. CMS',%
480 T50,'Z OHMS   DIA. CMS'//)
490 1100 FORMAT(1H ,T30,'MICROSTRIP TAPER'/T30,'----------------'//)
500 1200 FORMAT(///' IS ANOTHER RUN REQUIRED ? (NO=0,YES=1)')
510 10 WRITE(6,500)
520 3 READ(5,*)ITYPE
530 IF(ITYPE.EQ.1)GO TO 1
540 IF(ITYPE.EQ.2)GO TO 2
550 WRITE(6,600)
560 GO TO 3
570 1 WRITE(6,700)
580 WRITE(6,800)
590 READ(5,*)D1,E1,F1,Z01,ZT1,Y1,NSTEP1
600 WAVE1=2.998E10/(F1*SQRT(E1))
610 TLENG1=Y1*WAVE1
620 WRITE(6,900)E1,D1,F1,Y1,TLENG1
630 WRITE(6,1000)Y1,Z01,ZT1
640 NCHAN1=NSTEP1+1
650 DO 4 I1=1,NCHAN1
660 XL1=(I1-1)/(1.0*NSTEP1)
670 ZE1=Z01*EXP(XL1*ALOG(ZT1/Z01))
680 DE=D1/EXP(ZE1*SQRT(E1)/60.0)
690 ZH1=0.5*(ZT1+Z01)+0.5*(ZT1-Z01)*TANH(6.0*(XL1-0.5))
700 DH=D1/EXP(ZH1*SQRT(E1)/60.0)
```

```
710 ZP1=Z01+3.0*(ZT1-Z01)*XL1*XL1-2.0*(ZT1-Z01)*XL1*XL1*XL1
720 DP=D1/EXP(ZP1*SQRT(E1)/60.0)
730 X1=XL1*TLENG1
740 4 WRITE(6,300)X1,ZE1,DE,ZH1,DH,ZP1,DP
750 GO TO 5
760 2 WRITE(6,1100)
770 WRITE(6,100)
780 READ(5,*)H,E,T,F,Z0,ZT,Y,NSTEP
790 ZAV=SQRT(Z0*ZT)
800 CALL ZIMP(ZAV,E,H,T,WAV,M)
810 IF(M.EQ.1)GO TO 9
820 RAV=WAV/H
830 IF(RAV.LE.0.6)GO TO 6
840 RLAMDA=E/(1.0+0.63*(E-1.0)*(RAV**0.1255))
850 RATIO=SQRT(RLAMDA)
860 GO TO 7
870 6 RLAMDA=E/(1.0+0.6*(E-1.0)*(RAV**0.0297))
880 RATIO=SQRT(RLAMDA)
890 7 WAVE=2.998E10/(F*SQRT(E))
900 TLENG=Y*WAVE*RATIO
910 WRITE(6,400)E,H,T,F,Y,TLENG
920 WRITE(6,200)Y,Z0,ZT
930 NCHAN=NSTEP+1
940 DO 8 I=1,NCHAN
950 XL=(I-1)/(1.0*NSTEP)
960 ZE=Z0*EXP(XL*ALOG(ZT/Z0))
970 CALL ZIMP(ZE,E,H,T,WE,M)
980 IF(M.EQ.1)GO TO 9
990 ZH=0.5*(ZT+Z0)+0.5*(ZT-Z0)*TANH(6.0*(XL-0.5))
1000 CALL ZIMP(ZH,E,H,T,WH,M)
1010 IF(M.EQ.1)GO TO 9
1020 ZP=Z0+3.0*(ZT-Z0)*XL*XL-2.0*(ZT-Z0)*XL*XL*XL
1030 CALL ZIMP(ZP,E,H,T,WP,M)
1040 IF(M.EQ.1)GO TO 9
1050 X=XL*TLENG
1060 8 WRITE(6,300)X,ZE,WE,ZH,WH,ZP,WP
1070 5 WRITE(6,1200)
1080 11 READ(5,*)J
1090 IF(J.EQ.0)GO TO 9
1100 IF(J.EQ.1)GO TO 10
1110 WRITE(6,600)
1120 GO TO 11
1130 9 STOP
1140 END
1150 SUBROUTINE ZIMP(Z,E,H,T,W,M)
1160 100 FORMAT(1H ,T20,'NUMBER OF ALLOWED ITTERATIONS'/%
1170 T20,'IN COMPJTING LINE WIDTH IS EXCEEDED'///)
1180 L=1
1190 M=0
1200 STEP=0.1
1210 A=0.0
1220 B=377.0/SQRT(E)
1230 C=1.735*(E**(-0.0724))
1240 5 IF(L.GT.1000)GO TO 1
1250 A=A+STEP
1260 D=A**(-0.836)
1270 ZTEST=B/(A*(1.0+C*D))
1280 CHECK=(ZTEST-Z)/Z
1290 CHABS=ABS(CHECK)
1300 IF(CHABS.LE.0.01)GO TO 2
1310 IF(CHECK)3,2,4
1320 3 A=A-STEP
1330 STEP=STEP/10.0
1340 L=L+1
1350 GO TO 5
1360 4 L=L+1
1370 GO TO 5
1380 2 WUNCOR=A*H
1390 W=WUNCOR+(T*(ALOG(2.0*H/T)+1.0)/3.141592)
1400 GO TO 6
1410 1 M=1
1420 WRITE(6,100)
1430 6 RETURN
1440 END
```

Microstrip directional couplers

This article describes the properties of directional couplers and explains a procedure used to design microstrip directional couplers with the aid of the computer. The article also describes the experimental results obtained from six microstrip couplers, which were built to verify the computer program. The program is provided.

INTRODUCTION

Coupling between two microstrip lines relies on the proximity effect of two lines. The problem in designing coupled circuits in microstrip has been to analyse the 'odd mode' of propagation, where energy travelling down one microstrip line is coupled into a parallel line and travels in the reverse direction in that second line. Because the 'odd mode' gives tighter coupling than the 'even mode' in which the energy travels in the same direction after coupling, the 'odd mode' is the one most often used in coupled circuits.

There have been several papers written on this subject using a variety of techniques. Yamashita and Mittra (Ref. 1) present a variational method for the analysis of microstrip lines which can be extended to cover coupled lines. Stinehelfer (Ref. 2) describes an analytical program for calculating the field distribution about a microstrip line bounded by a shielding wall. The coupled line can be treated as a special case of this. On the other hand Bryant and Weiss (Ref. 3) try a theoretical analysis of microwave propagation in microstrip with particular reference to the case of coupled pairs of microstrip lines. Walters and Clar (Ref. 4) suggested a novel 'overlay' microstrip directional coupler, where extra coupling is obtained through a third conductor overlayed on top of the two main conductors and insulated from them: the advantage is that since most of the coupling is through the overlayed structure the dimensions of the coupler cease to be critical. The approach that Ramadan and Westgate (Ref. 5) use is based on treating the coupled microstrip lines as an electrostatic boundary value problem. A solution of Laplace's equation, subject to the appropriate boundary conditions, gives the potential at any point inside the boundary. The result is to produce equations for the odd and even mode cases which can be adapted for computation.

Finally Schwarzmann (Refs. 6 and 7) treats the problem in an original way by considering the even and odd modes separately and splitting the total capacitance in each case into a number of elementary components which can be computed using simple formulae. Schwarzmann's technique lends itself to relatively easy computation, unlike Ramadan's and Westgate's technique which involves infinite series.

The computer designs presented in this article are based on Schwarzmann's attractive solution to the problem.

OUTLINE OF THEORY

Even and odd mode in symmetrical networks

The problem of analysis of a symmetrical network can be tremendously simplified by the adoption of even and odd mode concept. Consider for example the symmetrical four port network of Fig. 1 with the symmetry plane indicated by the central line. Then if two signals of amplitude $\frac{1}{2}$ and both in phase are applied to ports 1 and 2, by symmetry a voltage maximum occurs at every point on the line of symmetry. On the symmetry plane $Z = \infty$, that is, the junction may be open circuited at the plane without affecting the field distribution, or alternatively a 'magnetic wall' may be located at this plane as shown in Fig. 2a. Similarly, if two signals of amplitude $\frac{1}{2}$ and out of phase are applied to ports 1 and 2, a voltage minimum occurs on the line of symmetry. On the symmetry plane $Z = 0$, that is, a short circuit (an 'electric wall') may be located at the plane without affecting the field distributions, as shown in Fig. 2b. These two modes of operation of the network are called the even and odd modes, respectively.

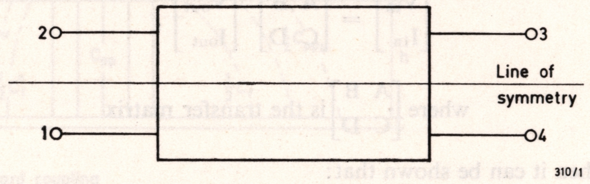

Fig. 1—Symmetrical four port network

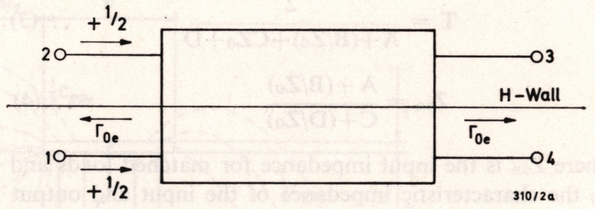

Fig. 2a—Even mode excitation

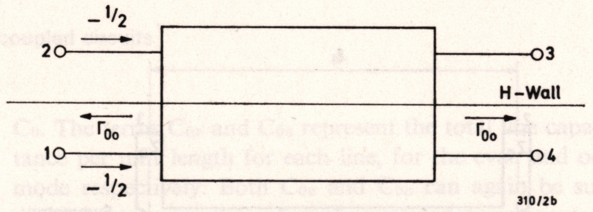

Fig. 2b—Odd mode excitation

By superposition, the sum of the two mode field distributions corresponds to that given by a signal of unit amplitude input at port 1. The resultant signals out of each port are also given by the superposition of those obtained in the even and odd modes. For the even mode a reflection coefficient Γ_{0e} and a transmission coefficient T_{0e} are determined, and similarly for the odd mode, Γ_{0o} and T_{0o} are determined. Superposition gives the following amplitudes of the signals emerging from the four ports:

$$\left.\begin{aligned} b_1 &= \tfrac{1}{2}(\Gamma_{0e}+\Gamma_{0o}) \\ b_2 &= \tfrac{1}{2}(\Gamma_{0e}-\Gamma_{0o}) \\ b_3 &= \tfrac{1}{2}(T_{0e}-T_{0o}) \\ b_4 &= \tfrac{1}{2}(T_{0e}+T_{0o}) \end{aligned}\right\} \quad \ldots(1)$$

The reflection and transmission coefficients can be derived from the circuit transfer matrix. For a general network:

$$\begin{bmatrix} V_{in} \\ I_{in} \end{bmatrix} = \begin{bmatrix} A & B \\ C & D \end{bmatrix} \begin{bmatrix} V_{out} \\ I_{out} \end{bmatrix},$$

where $\begin{bmatrix} A & B \\ C & D \end{bmatrix}$ is the transfer matrix

Then it can be shown that:

$$\Gamma = \frac{A+(B/Z_0)-CZ_0-D}{A+(B/Z_0)+CZ_0+D} \quad \ldots(2)$$

$$T = \frac{2}{A+(B/Z_0)+CZ_0+D} \quad \ldots(3)$$

$$Z_{in} = \frac{A+(B/Z_0)}{C+(D/Z_0)} \quad \ldots(4)$$

where Z_{in} is the input impedance for matched loads and Z_0 the characteristic impedance of the input and output ports.

Consider the directional coupler of Fig. 3, consisting of two identical lines 1–4 and 2–3 with uniform spacing over the electrical length θ. The lines are terminated by input and output lines of characteristic impedance Z_0. Applying the even and odd mode concept to the coupler and defining V_1,I_1 as the input voltage and current at port 1 and V_4,I_4 as the output voltage and current at port 4, with subscripts e and o referring to the even and odd mode excitations respectively, then for the even mode the transfer matrix equation is:

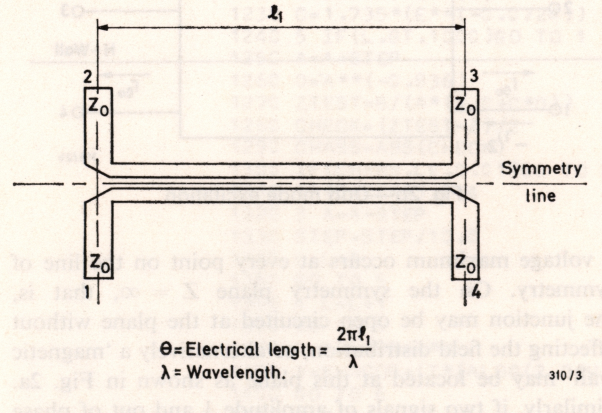

Fig. 3—Directional coupler

$$\begin{bmatrix} V_{1e} \\ I_{1e} \end{bmatrix} = \begin{bmatrix} \cos\theta_e & j\,Z_{0e}\sin\theta_e \\ (j/Z_{0e})\sin\theta_e & \cos\theta_e \end{bmatrix} \begin{bmatrix} V_{4e} \\ I_{4e} \end{bmatrix} \quad \ldots(5)$$

and for the odd mode:

$$\begin{bmatrix} V_{1o} \\ I_{1o} \end{bmatrix} = \begin{bmatrix} \cos\theta_o & j\,Z_{0o}\sin\theta_o \\ (j/Z_{0o})\sin\theta_o & \cos\theta_o \end{bmatrix} \begin{bmatrix} V_{4o} \\ I_{4o} \end{bmatrix} \quad \ldots(6)$$

where Z_{0e} and Z_{0o} are the even and odd mode impedances, respectively.

In the case where the electrical lengths of the even and odd modes are equal, then

$$\theta_e = \theta_o = \theta = \frac{2\pi\ell_1}{\lambda} \quad \ldots(7)$$

where ℓ_1 is the length of the lines and λ the wavelength.

By using Eqs. 1, 2, 3 and 4 when the condition

$$Z_0 = (Z_{0e}.Z_{0o})^{\frac{1}{2}} \quad \ldots(8)$$

is satisfied, Eqs. 5 and 6 can be manipulated to yield:

$$b_1 = 0 \quad \ldots(9)$$

$$b_2 = \Gamma_{0e} = \frac{j[(Z_{0e}/Z_{0o})^{\frac{1}{2}}-(Z_{0o}/Z_{0e})^{\frac{1}{2}}]\sin\theta}{2\cos\theta+j[(Z_{0e}/Z_{0o})^{\frac{1}{2}}+(Z_{0o}/Z_{0e})^{\frac{1}{2}}]\sin\theta} \quad \ldots(10)$$

$$b_3 = 0 \quad \ldots(11)$$

$$b_4 = T_{0e} = \frac{2}{2\cos\theta+j[(Z_{0e}/Z_{0o})^{\frac{1}{2}}+(Z_{0o}/Z_{0e})^{\frac{1}{2}}]\sin\theta} \quad \ldots(12)$$

which represent the signals emerging from the four arms for a unit input into port 1.

Eqs. 9, 10, 11 and 12 show that the coupler is perfectly matched and isolated ($b_3 = 0$), and that the phase difference between waves b_2 and b_4 is 90° at all frequencies. The coupling to port 2 is a maximum when sin θ = 1, that is, the line length is an odd multiple of a quarter wavelength, giving a maximum voltage coupling:

$$k = \frac{Z_{0e}/Z_{0o}-1}{Z_{0e}/Z_{0o}+1} \quad \ldots(13)$$

The coupling to port 2 is zero when the line length is an integral multiple of a half-wavelength.

Having decided on the coupling required and the impedance of the coupler Z_0, Eqs. 8 and 13 will give the required values for Z_{0e} and Z_{0o}.

Determination of the even and odd mode impedances for microstrip

The characteristic impedance of microstrip can be calculated with the elementary transmission line equation:

$$Z_0 = \frac{1}{vC_0} \quad \ldots(14)$$

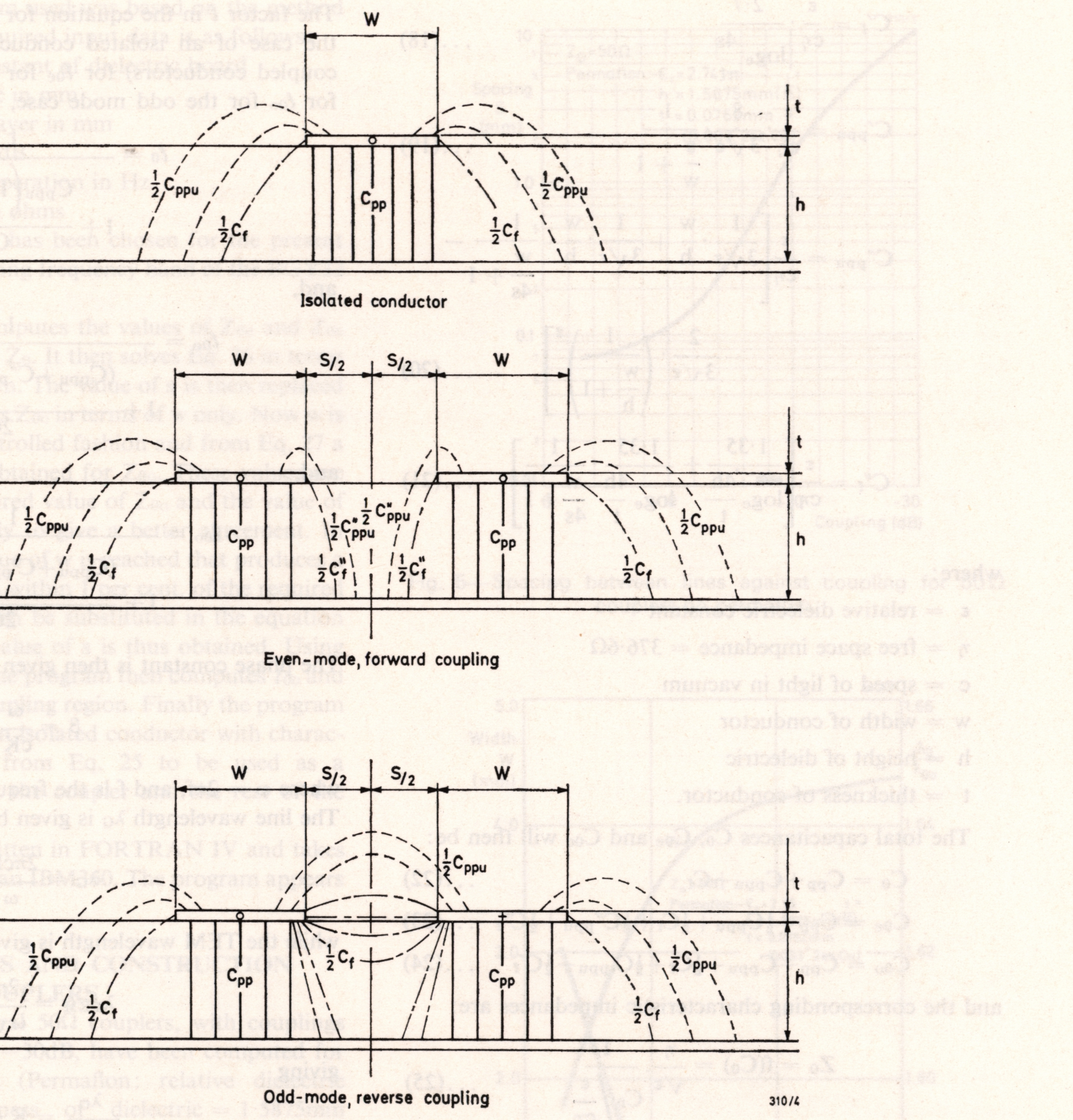

Fig. 4—Microstrip coupled circuits

where v is the velocity of propagation down the line and C_0 the capacitance per unit length.

The capacitance C_0, for microstrip, cannot be calculated directly without using infinite series, and so Schwarzmann suggested (Refs. 6 and 7) subdividing the total capacitance into three easily analysed components—the parallel plate capacitance C_{pp} between the lower surface of the conductor and the ground plane, the fringing capacitance C_f at the edges of the conductor, and the capacitance between the upper surface of the conductor and the ground plane C_{ppu}.

When a second conductor is introduced close to the first one, the field distribution changes. In the even mode, the electric field lines follow a pattern similar to that of the isolated conductor. In the odd mode, the two conductors are linked by the field lines.

Eq. 14 can be employed to find the characteristic impedance of each of the coupled lines with C_{0e} and C_{0o} used for the even and odd modes respectively in place of C_0. The terms C_{0e} and C_{0o} represent the total line capacitance per unit length for each line, for the even and odd mode respectively. Both C_{0e} and C_{0o} can again be subdivided into a number of easily analysed components.

These capacitance components for the isolated line, and even and odd modes of two coupled lines are shown in Fig. 3. Schwarzmann gives approximate formulae from which all the capacitance components can be calculated. These are as follows:

$$C_{pp} = \frac{\varepsilon}{c\eta}.\frac{w}{h} \quad \ldots(15)$$

$$C_{ppu} = \frac{\varepsilon}{c\eta}\cdot\frac{2}{3\sqrt{\varepsilon}}\,\frac{w}{h}\left(\frac{1}{\frac{w}{h}+1}\right)^2 \quad \ldots(16)$$

$$C_f = \frac{\varepsilon}{c\eta}\cdot\frac{2{\cdot}7}{\log_e\frac{4h}{t}} \quad \ldots(17)$$

$$C'_f = \frac{\varepsilon}{c\eta}\cdot\frac{2{\cdot}7}{\log_e\dfrac{4s}{\pi t}} \qquad \ldots(18)$$

$$C'_{ppu} = \frac{\varepsilon}{c\eta}\cdot\frac{8}{3\sqrt{\varepsilon}}\cdot\frac{1}{\dfrac{s}{w}+1} \qquad \ldots(19)$$

$$C''_{ppu} = \frac{\varepsilon}{c\eta}\left[\frac{1}{3\sqrt{\varepsilon}}\cdot\frac{w}{h}+\frac{1}{3\sqrt{\varepsilon}}\cdot\frac{w}{h}\cdot\frac{1}{\dfrac{w}{4s}+1}-\frac{2}{3\sqrt{\varepsilon}}\cdot\left(\frac{1}{\dfrac{w}{h}+1}\right)^2\right] \qquad \ldots(20)$$

$$C''_f = \frac{\varepsilon}{c\eta}\left[\frac{1{\cdot}35}{\log_e\dfrac{4h}{t}}+\frac{1{\cdot}35}{\log_e\dfrac{4h}{t}}\cdot\frac{1}{\dfrac{w}{4s}+1}\right] \qquad \ldots(21)$$

where:

ε = relative dielectric constant

η = free space impedance = 376·6Ω

c = speed of light in vacuum

w = width of conductor

h = height of dielectric

t = thickness of conductor.

The total capacitances C_0, C_{0e} and C_{0o} will then be:

$$C_0 = C_{pp}+C_{ppu}+C_f \qquad \ldots(22)$$

$$C_{0e} = C_{pp}+\tfrac{1}{2}C_{ppu}+\tfrac{1}{2}C_f+\tfrac{1}{2}C''_{ppu}+\tfrac{1}{2}C''_f \qquad \ldots(23)$$

$$C_{0o} = C_{pp}+C_{ppu}+\tfrac{1}{2}C_f+\tfrac{1}{2}C'_{ppu}+\tfrac{1}{2}C'_f \qquad \ldots(24)$$

and the corresponding characteristic impedances are:

$$Z_0 = f(C_0) = \frac{\eta}{\sqrt{\varepsilon}}\cdot\frac{1}{C_0\Big/\dfrac{\varepsilon}{c\eta}} \qquad \ldots(25)$$

$$Z_{0e} = f(C_{0e}) = \frac{\eta}{\sqrt{\varepsilon}}\cdot\frac{1}{C_{0e}\Big/\dfrac{\varepsilon}{c\eta}} \qquad \ldots(26)$$

$$Z_{0o} = f(C_{0o}) = \frac{\eta}{\sqrt{\varepsilon}}\cdot\frac{1}{C_{0o}\Big/\dfrac{\varepsilon}{c\eta}} \qquad \ldots(27)$$

With part of the electric field in air and the rest in the dielectric the velocity of propagation in microstrip is not a simple constant. To find the wavelength along the line, which will determine the length of resonant sections, the free-space value of propagation velocity must be adjusted to account for the heterogeneity. This is done by including the effects of the air-dielectric in a multiplying factor K for the velocity in free space c, in the equation

$$v = cK \qquad \ldots(28)$$

where v is the line velocity and K is given by

$$K = \frac{1}{\sqrt{1+\ell^2(\varepsilon-1)}} \qquad \ldots(29)$$

The factor ℓ in the equation for K is substituted for ℓ_0 in the case of an isolated conductor, and (in the case of coupled conductors) for ℓ_{0e} for the even mode case and for ℓ_{0o} for the odd mode case, where:

$$\ell_0 = \frac{1}{1+\dfrac{C_{ppu}\left(1-\dfrac{1}{\sqrt{\varepsilon}}\right)}{C_0}}, \qquad \ldots(30)$$

and,

$$\ell_{0e} = \frac{1}{1+\dfrac{(C_{ppu}+C''_{ppu})\left(1-\dfrac{1}{\sqrt{\varepsilon}}\right)}{2C_{0e}}}, \qquad \ldots(31)$$

and,

$$\ell_{0o} = \frac{1}{1+\dfrac{(C_{ppu}+C'_{ppu})\left(1-\dfrac{1}{\sqrt{\varepsilon}}\right)}{2C_{0o}}} \qquad \ldots(32)$$

The phase constant is then given by

$$\beta = \frac{\omega}{cK} \qquad \ldots(33)$$

where $\omega = 2\pi f$, and f is the frequency.
The line wavelength λ_G is given by

$$\lambda_G = \frac{2\pi cK}{\omega} \qquad \ldots(34)$$

while the TEM wavelength is given by

$$\lambda_{TEM} = \frac{2\pi c}{\omega\sqrt{\varepsilon}}, \qquad \ldots(35)$$

giving

$$\frac{\lambda_G}{\lambda_{TEM}} = K\sqrt{\varepsilon}. \qquad \ldots(36)$$

DESIGN PROCEDURE AND COMPUTATIONAL METHOD

The theory described above can be readily used to design microstrip couplers. Once the required coupling k and coupler impedance Z_0 have been decided, then Eqs. 8 and 13 will give the required values for the even and odd mode characteristic impedances Z_{0e} and Z_{0o}. Then by replacing the capacitance components in Eqs. 26 and 27 and by solving these for w and s (the width of the lines and the spacing between the lines) two of the dimensions of the coupler will be calculated. The third, the length of the coupling region, can be computed from Eqs. 29, 32 and 34. Note that the length of the coupling region (a quarter wavelength) depends on the degree of coupling. The odd mode of coupling is chosen (by using ℓ_{0o} in Eq. 29) where energy travelling down one microstrip line is coupled into a parallel line and travels in the reverse direction in that second line. The odd mode gives tighter coupling than the even, in which energy travels in the same direction after coupling.

The computer program used was based on the method described above. The required input data is as follows:
1) Relative dielectric constant of dielectric board
2) Thickness of dielectric in mm
3) Thickness of copper layer in mm
4) Coupling required in dB
5) Centre frequency of operation in Hz
6) Coupler impedance in ohms

The centre frequency has been chosen for the present work to fall in the operating frequency band of the BGY22 and BGY23 amplifier.

The program first computes the values of Z_{0e} and Z_{0o} from the values of k and Z_0. It then solves Eq. 26 in terms of s, assuming w is known. The value of s is then replaced in Eq. 27 which now gives Z_{0o} in terms of w only. Now w is allowed to vary in a controlled fashion and from Eq. 27 a series of test values is obtained for Z_{0o}. These values are compared with the required value of Z_{0o} and the value of w is changed accordingly to give a better agreement. In this way eventually a value of w is reached that produces a test value of Z_{0o} which is within 1 per cent. of the required value. This value can then be substituted in the equation for s and the required value of s is thus obtained. Using these values of w and s the program then computes ℓ_{0o} and then the length of the coupling region. Finally the program computes the width of an isolated conductor with characteristic impedance Z_0, from Eq. 25 to be used as a connecting line between the coupler and the rest of the circuitry.

The program was written in FORTRAN IV and takes 2 to 3 seconds to run on an IBM360. The program appears on page 186.

COMPUTED RESULTS AND CONSTRUCTION OF MICROSTRIP COUPLERS

The dimensions of several 50Ω couplers, with couplings varying from −3dB to −30dB, have been computed for Permaflon at 470MHz (Permaflon: relative dielectric constant = 2·74, thickness of dielectric = 1·5875mm ($\frac{1}{16}$″), thickness of copper layer = 0·0762mm (0·003″, 2 oz. Cu)). The computed results are shown on Figs. 5 and 6. Fig. 5 gives the spacing between the lines plotted against the coupling while Fig. 6 gives the width of the lines, w, and the ratio of the free space wavelength λ_0 to the odd mode wavelength λ_{0o} in the dielectric, against the coupling. It is interesting to observe that there is a minimum in the curve for λ_0/λ_{0o} occurring at a coupling of about −17dB and that the curve is asymmetrical about the minimum.

The computed dimensions for the six couplers that were built in microstrip are given in Table 1 together with the measured dimensions of the couplers which were built. Fig. 7 shows the shape of the coupler and details of the corner which is the transition from a width w_0 (corresponding to the characteristic impedance Z_0 of an isolated conductor) to a width w which is the coupler line width. The connections to the four arms of the coupler were made through the board using General–Radio connectors, as shown in Fig. 8.

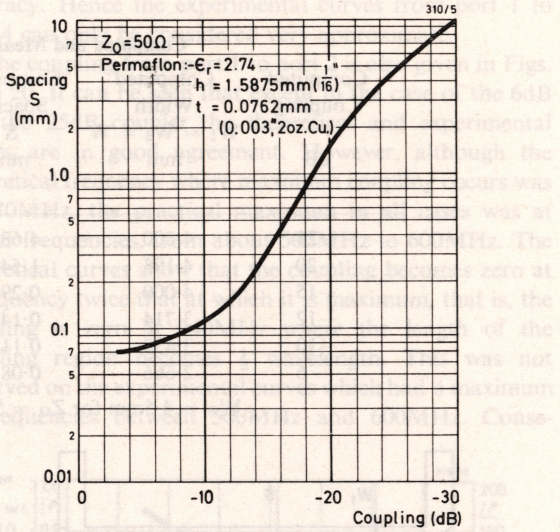

Fig. 5—Spacing between lines against coupling for 50Ω couplers on permaflon.

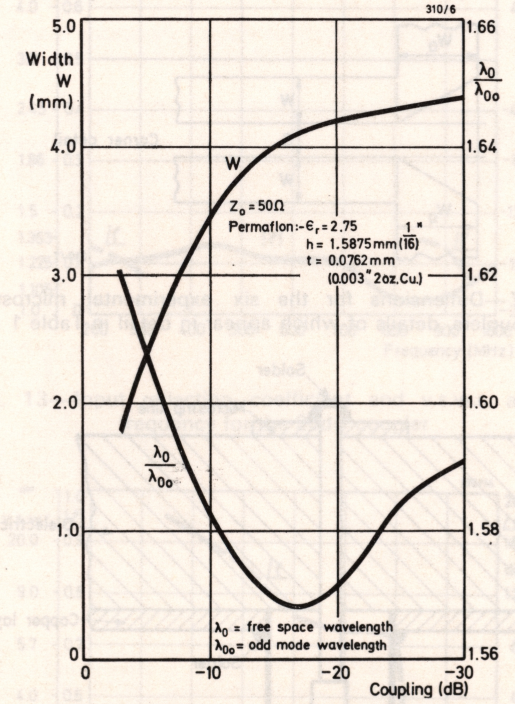

Fig. 6—Width of lines and ratio λ_0/λ_{0o} against coupling for 50Ω couplers on permaflon.

THE EXPERIMENTAL RESULTS

The properties of the couplers were measured on the Hewlett Packard Microwave Network Analyser. The transmission to ports 2, 3, 4 and the reflection at port 1, for a signal into port 1, were measured. Since only two ports were involved in each measurement, the remaining two ports were terminated to 50Ω loads. The port numbers correspond to those in Fig. 3. Thus for an input at port 1, port 2 is the coupled port and port 3 is the isolated port.

The results are plotted in Figs. 9 to 21. The magnitude and phase of the reflection coefficient against the frequency is given in Figs. 9 to 14 for the various couplers. A v.s.w.r.

TABLE I

Computed and Measured Dimensions for Coupler in Fig. 7

Computed Coupling dB	Computed Width $W_1 = W_2 = W$ mm	Computed Spacing S mm	Computed Length l mm	Measured Width W_1 mm Average	Measured Width W_2 mm Average	Measured Spacing S mm Average
−25	4·300	4·688	100·800	4·112	4·117	4·866
−20	4·193	1·548	101·457	3·990	4·004	1·739
−15	4·000	0·298	101·635	3·805	3·795	0·476
−12	3·714	0·145	101·198	3·517	3·526	0·327
−10	3·438	0·111	100·775	3·263	3·273	0·277
− 6	2·666	0·081	99·589	2·523	2·509	0·228

$W_O = 4{\cdot}5$mm for $Z_O = 50\Omega$ Accuracy of measurements ±10μm

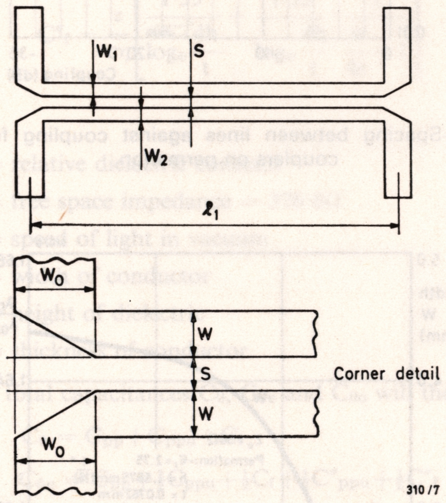

Fig. 7—Dimensions for the six experimental microstrip couplers, details of which appear in detail in Table 1

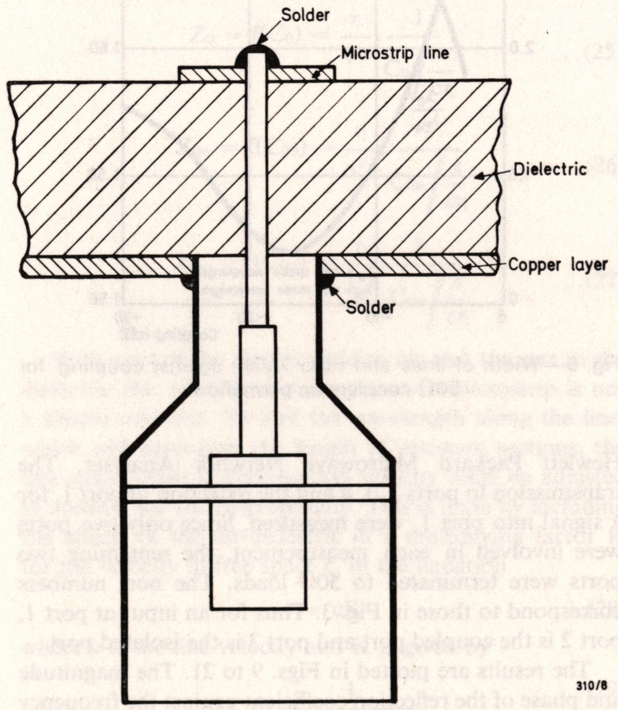

Fig. 8—Through-the-board connection to microstrip lines

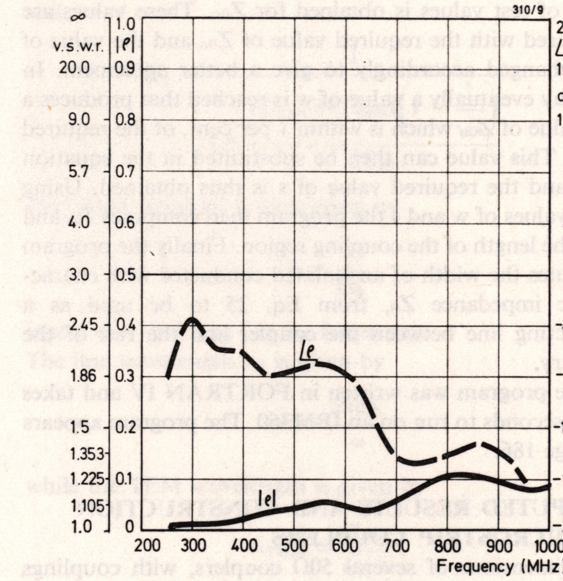

Fig. 9—Input reflection coefficient and v.s.w.r. against frequency for the 6dB coupler

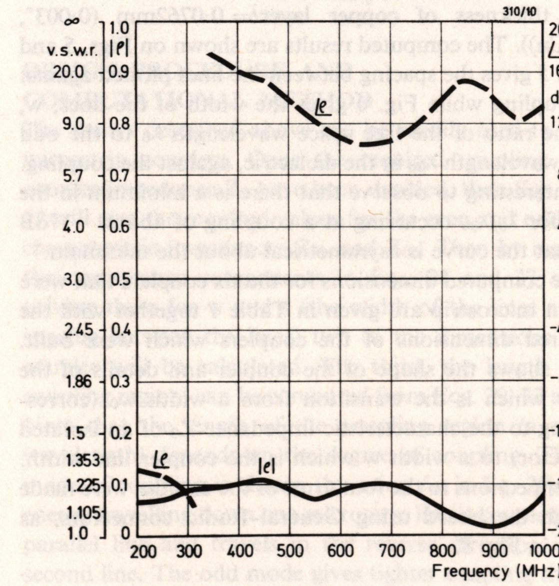

Fig. 10—Input reflection coefficient and v.s.w.r. against frequency for the 10dB coupler

scale is also given in these graphs. The results are similar in all cases with maximum reflection coefficient 0·15 (v.s.w.r. = 1·353) in the case of the 12dB coupler. (For comparison, the theoretical reflection coefficient = 0 or v.s.w.r. = 1, at all frequencies).

Figs. 15 to 20 give the theoretical and experimental frequency responses at ports 2, 3, 4 for an input at port 1. The theoretical curve for the transmission between port 1 and port 3 should be at infinity since the two ports are, theoretically, perfectly isolated. In practice the isolation was found to vary from one coupler to the other but it was always better than 18dB.

The transmission loss from port 1 to port 4 was small (less than 1·0dB in most cases) and it was difficult to measure on the Microwave Network Analyser, with any accuracy. Hence the experimental curves from port 1 to port 4 can only be considered very approximate.

The coupling from port 1 to port 2 is also given in Figs. 15 to 20. It can be seen that except in the case of the 6dB and the 25dB coupler the theoretical and experimental curves are in good agreement. However, although the theoretical frequency where maximum coupling occurs was at 470MHz, the practical maximum in all cases was at higher frequencies, from about 500MHz to 600MHz. The theoretical curves show that the coupling becomes zero at a frequency twice that at which it is maximum, that is, the coupling is zero at 940MHz where the length of the coupling region becomes ½ wavelength. This was not observed on the experimental curves which had a maximum at frequencies between 500MHz and 600MHz. Conse-

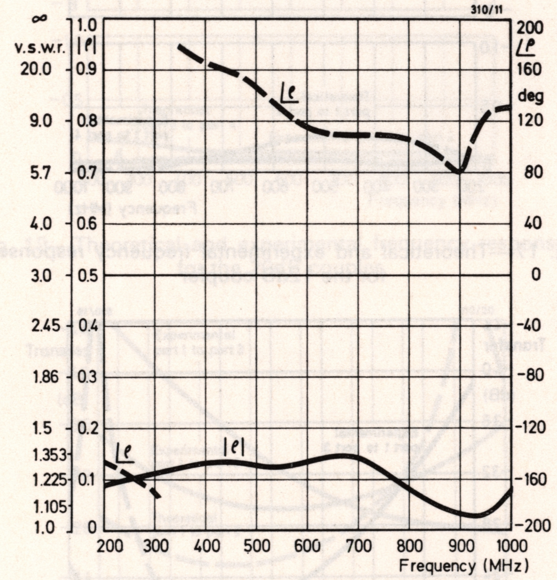

Fig. 11—Input reflection coefficient and v.s.w.r. against frequency for the 12dB coupler

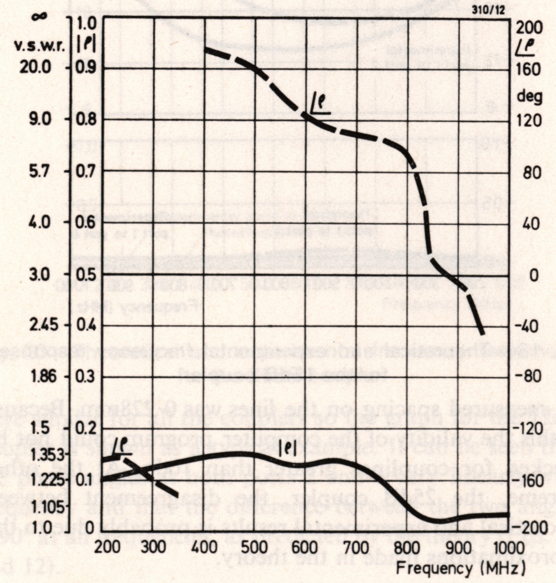

Fig. 12—Input reflection coefficient and v.s.w.r. against frequency for the 15dB coupler

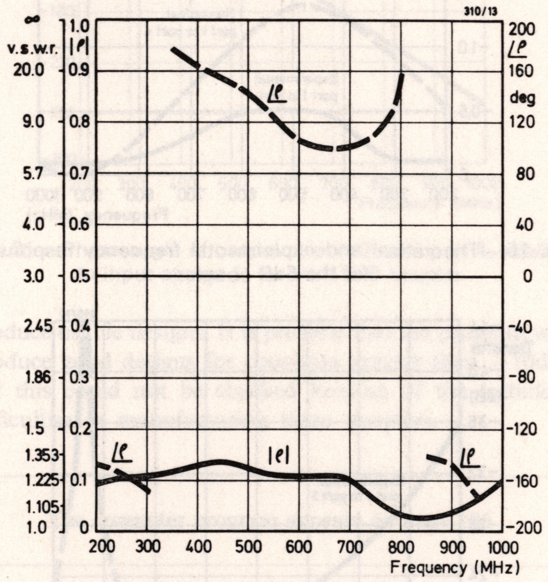

Fig. 13—Input reflection coefficient and v.s.w.r. against frequency for the 20dB coupler

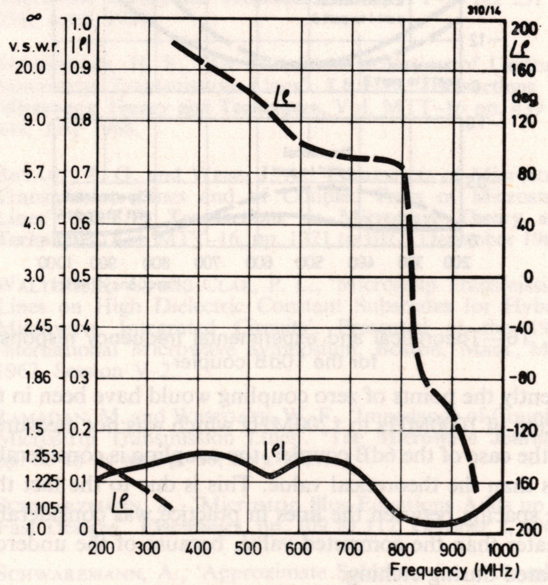

Fig. 14—Input reflection coefficient and v.s.w.r. against frequency for the 25dB coupler

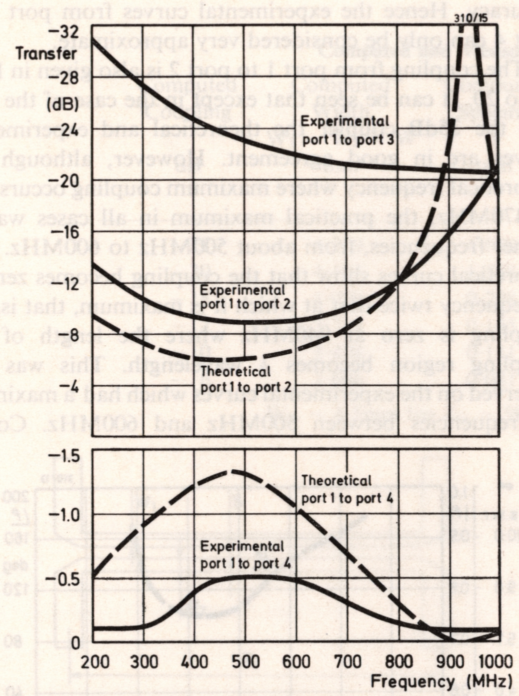

Fig. 15—Theoretical and experimental frequency responses, for the 6dB coupler

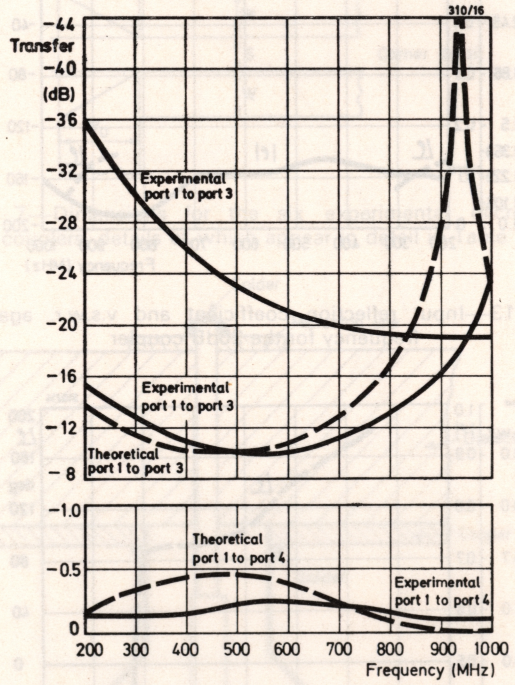

Fig. 16—Theoretical and experimental frequency responses, for the 10dB coupler

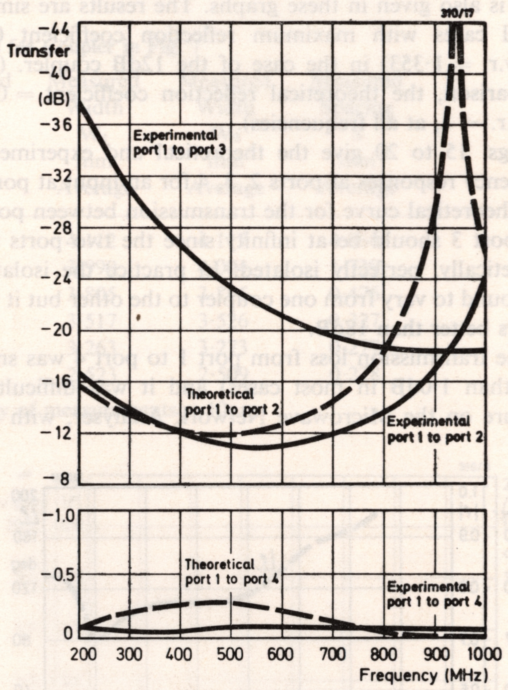

Fig. 17—Theoretical and experimental frequency responses, for the 12dB coupler

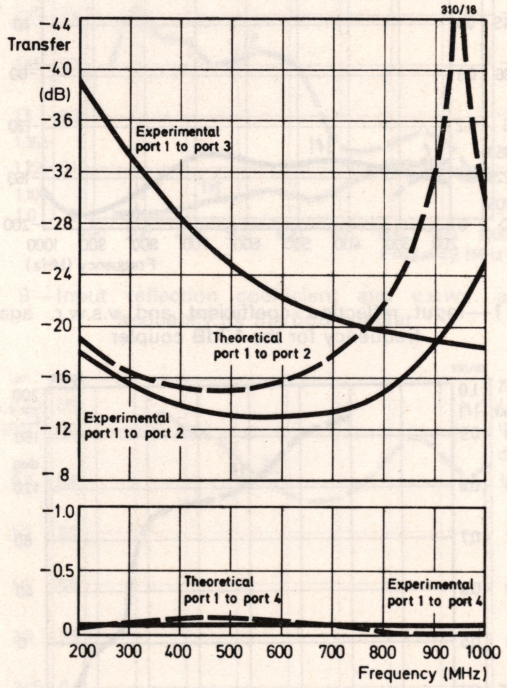

Fig. 18—Theoretical and experimental frequency responses, for the 15dB coupler

quently the points of zero coupling would have been in the region of 1000MHz to 1200MHz which was not measured. In the case of the 6dB coupler, the coupling is considerably less than the theoretical value. This is due to the fact that the spacing between the lines in practice was considerably greater than the computed value, because of the undercut created during etching.

In fact where the theoretical spacing should be 0·081mm the measured spacing on the lines was 0·228mm. Because of this the validity of the computer program could not be checked for couplings greater than 10db. At the other extreme, the 25dB coupler, the disagreement between theoretical and experimental results is probably due to the approximations made in the theory.

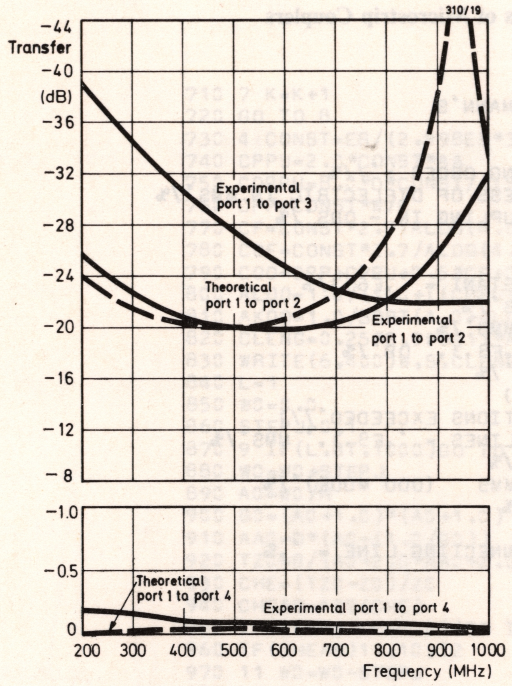

Fig. 19—Theoretical and experimental frequency responses, for the 20dB coupler

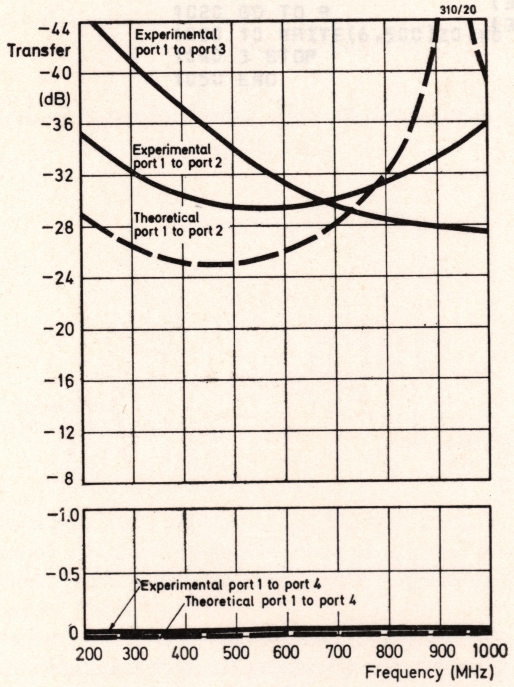

Fig. 20—Theoretical and experimental frequency responses, for the 25dB coupler

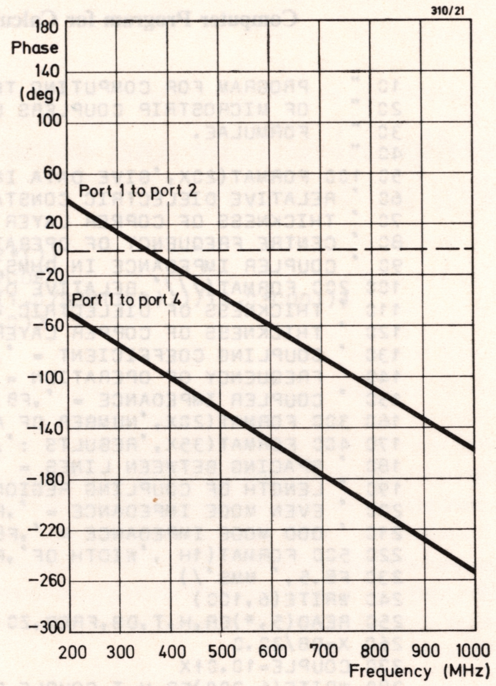

Fig. 21—Phase angle of output at port 2, and port 4, relative to input at port 1, for the 12dB coupler

Finally Fig. 21 gives the phase angle at ports 2 and 4 relative to that at port 1 for the 12dB coupler. The results were similar for all the couplers so the graph for the 12dB coupler is shown as a typical example. It can be seen that the phase angles at both ports 2 and 4 vary linearly with frequency and that the difference between the two angles is 90° at all frequencies, as predicted by the theory (Eqs. 10 and 12).

It can be seen that in cases where couplings of 10 to 20dB are required the computer program developed will produce usable designs. It is possible that the program will produce good designs for couplings greater than −10dB, but this could not be checked because of the technical difficulties in manufacturing these couplers.

The computer program appears on page 186

REFERENCES

1. Yamashita, E. and Mittra, R., 'Variational Method for the Analysis of Microstrip Lines'. **I.E.E.E. Transactions on Microwave Theory and Techniques,** Vol. MTT–16 pp. 251 to 256, April 1969.

2. Stinehelfer, H. E., 'An Accurate Calculation of Uniform Microstrip Transmission Lines'. **I.E.E.E. Transactions on Microwave Theory and Techniques,** Vol. MTT–16 pp. 439 to 444, July 1968.

3. Bryant, T. G. and Weiss, J. A., 'Parameters of Microstrip Transmission Lines and of Coupled Pairs of Microstrip Lines', **I.E.E.E. Transactions on Microwave Theory and Techniques,** Vol. MTT–16, pp. 1021 to 1027, December 1968.

4. Walters, K. C. and Clar, P. L., 'Microstrip Transmission Lines on High Dielectric Constant Substrates for Hybrid Microwave Integrated Circuits'. Presented at the 1967 International Microwave Symposium, Boston, Mass., May 1967, Session V–2.

5. Ramadan, M. and Westgate, W. F., 'Impedance of Coupled Microstrip Transmission Lines'. **'The Microwave Journal',** pp. 30 to 34 and p. 56, July 1971.

6. Schwarzmann, A., 'Microstrip Plus Equations Adds up to Fast Designs'. **Electronics,** pp. 109 to 112, October 2, 1967.

7. Schwarzmann, A., 'Approximate Solutions for a Coupled Pair of Microstrip Lines in Microwave Integrated Circuits'. **The Microwave Journal,** pp. 79 to 82, May 1969.

Computer Program for Calculating Dimensions of Microstrip Couplers

```
10 "    PROGRAM FOR COMPUTING THE DIMENSIONS
20 "    OF MICROSTRIP COUPLERS USING SCHWARZMANN'S
30 "    FORMULAE.
40 "
50 100 FORMAT(20X,'GIVE DATA IN THE FOLLOWING ORDER :'//%
60 ' RELATIVE DIELECTRIC CONSTANT'/' THICKNESS OF DIELECTRIC IN MMS'/%
70 ' THICKNESS OF COPPER LAYER IN MMS'/' COUPLING IN - DBS'/%
80 ' CENTRE FREQUENCY OF OPERATION IN HZ'/%
90 ' COUPLER IMPEDANCE IN OHMS'///)
100 200 FORMAT(///' RELATIVE DIELECTRIC CONSTANT = ',F6.3/%
110 ' THICKNESS OF DIELECTRIC = ',F8.5,' MMS'/%
120 ' THICKNESS OF COPPER LAYER = ',F8.5,' MMS'/%
130 ' COUPLING COEFFICIENT = ',F8.5,'    OR',F8.3,' DB'/%
140 ' FREQUENCY OF OPERATION = ',E10.3,' HZ'/%
150 ' COUPLER IMPEDANCE = ',F8.3,' OHMS'///)
160 300 FORMAT(20X,'NUMBER OF ALLOWED ITERATIONS EXCEEDED'//)
170 400 FORMAT(35X,'RESULTS :'//' WIDTH OF LINES = ',F8.3,' MMS'/%
180 ' SPACING BETWEEN LINES = ',F8.3,' MMS'/%
190 ' LENGTH OF COUPLING REGION = ',F8.3,' MMS    (ODD MODE)'/%
200 ' EVEN MODE IMPEDANCE = ',F8.3,' OHMS'/%
210 ' ODD MODE IMPEDANCE = ',F8.3,' OHMS'/)
220 500 FORMAT(1H ,'WIDTH OF',F8.3,' OHM CONNECTING LINE = ',%
230 F8.5,' MMS'/)
240 WRITE(6,100)
250 READ(5,*)ER,H,T,DB,FREQ,Z0
260 X=DB/20.0
270 COUPLE=10.0↑X
280 WRITE(6,200)ER,H,T,COUPLE,DB,FREQ,Z0
290 B=376.6/SQRT(ER)
300 D=1.0/(3.0*SQRT(ER))
310 F=1.35/ALOG(4.0*H/T)
320 ZOE=Z0*SQRT(1.0+COUPLE)/SQRT(1.0-COUPLE)
330 ZOO=Z0*SQRT(1.0-COUPLE)/SQRT(1.0+COUPLE)
340 K=1
350 W=0.0
360 M=0
370 STEP=0.01
380 8 IF(K.GT.1000)GO TO 1
390 GO TO 2
400 1 WRITE(6,300)
410 GO TO 3
420 2 W=W+STEP
430 A=W/H
440 G=(A+1.0)*(A+1.0)
450 AA=D*(A-(1.0/G))
460 BB=D/G
470 CC=A+AA+0.5*D*A-BB+1.5*F
480 DD=0.5*D*A+0.5*F
490 X=((B/ZOE)-CC)/DD
500 Y=1.0/X
510 XX=4.0*(Y-1.0)
520 S=W/XX
530 IF(S)13,13,14
540 13 TESZOO=1.0E10
550 GO TO 15
560 14 ZCPPU=2.0*AA
570 M=M+1
580 ZCPPUD=4.0*D/((S/W)+1.0)
590 ZCDF=1.35/ALOG(4.0*S/(3.141592*T))
600 TESZOO=B/(A+ZCPPU+F+ZCPPUD+ZCDF)
610 IF(M.EQ.1)STEP=STEP/10.0
620 15 CHECK=(TESZOO-ZOO)/ZOO
630 CHABS=ABS(CHECK)
640 IF(CHABS.LE.0.01)GO TO 4
650 IF(CHECK)5,4,7
660 IF(M.EQ.1)STEP=STEP*10.0
670 5 W=W-STEP
680 STEP=STEP/10.0
690 K=K+1
700 GO TO 8
```

```
710 7 K=K+1
720 GO TO 8
730 4 CONST=ER/(2.998E8*376.6)
740 CPPU=2.0*CONST*AA
750 CDPPU=8.0*D*CONST/((S/W)+1.0)
760 CPP=CONST*W/H
770 CF=CONST*2.7/ALOG(4.0*H/T)
780 CDF=CONST*2.7/ALOG(4.0*S/(3.141592*T))
790 COO=CPP+CPPU+0.5*CF+0.5*CDPPU+0.5*CDF
800 ALOO=1.0/(1.0+((CPPU+CDPPU)*(1.0-(1.0/SQRT(ER)))/(2.0*COO)))
810 AKOO=1.0/SQRT(1.0+ALOO*ALOO*(ER-1.0))
820 CLENG=0.25*2.998E11*AKOO/FREQ
830 WRITE(6,400)W,S,CLENG,ZOE,ZOO
840 L=1
850 W0=0.0
860 STEPJ=0.1
870 9 IF(L.GT.1000)GO TO 1
880 W0=W0+STEPJ
890 A0=W0/H
900 G0=(A0+1.0)*(A0+1.0)
910 AA0=D*(A0-(1.0/G0))
920 TZ0=B/(A0+2.0*AA0+2.0*F)
930 CHE=(TZ0-Z0)/Z0
940 CHEAB=ABS(CHE)
950 IF(CHEAB.LE.0.01)GO TO 10
960 IF(CHEAB)11,10,12
970 11 W0=W0-STEPJ
980 STEPJ=STEPJ/10.0
990 L=L+1
1000 GO TO 9
1010 12 L=L+1
1020 GO TO 9
1030 10 WRITE(6,500)Z0,W0
1040 3 STOP
1050 END
```

Interdigital filters and experimental microstrip filter design at 470MHz

Design techniques for interdigital microstrip filters are briefly surveyed. As an example, the design and construction of an experimental microstrip filter with a Chebychev response and a passband centred on 470MHz is described. The filter has an insertion loss of 0.5dB and gives an attenuation of 60dB at 300MHz and 650MHz, and 20dB at 400MHz and 550MHz.

INTRODUCTION

Interdigital filters are very attractive propositions at microwave frequencies because of their interesting band-pass properties. The main advantages of interdigital filters over other filters (Ref. 1) are as follows.

1) They are very compact.

2) The tolerances required in their manufacture are relatively relaxed because of the comparatively large spacings between the resonator elements.

3) The second passband is centred at three times the frequency of the first passband and there is therefore no possibility of spurious responses at frequencies between the bands.

4) The rates of cut-off and attenuation of the stop-bands are high.

5) Interdigital filters can be fabricated easily either in microstrip, or in self-supporting structural forms in which dielectric material need not be used. Thus dielectric losses can be minimised.

Approximate design techniques for interdigital filters have been described by Matthaei (Ref. 1) and have been used to design both narrowband and wideband filters. Matthaei extends the theory for parallel coupled resonators which are $\lambda_0/2$ long at the midband frequency (Ref. 2), making certain assumptions and approximations. He derives an interdigital filter from a parallel coupled $\lambda_0/2$ resonator filter by assuming that each resonator is cut in the middle and folded double.

OUTLINE OF THE THEORY BY MATTHAEI

Fig. 1 shows one type of filter design suitable for narrow to moderate bandwidth (30% or less relative to midband). The structure consists of TEM mode strip-line resonators, one quarter wavelength long at the midband frequency, short-circuited at one end and open-circuited at the other. Coupling is achieved through the fields fringing adjacent resonator elements. Each element serves as a resonator except for the input and output elements which are used for impedance matching.

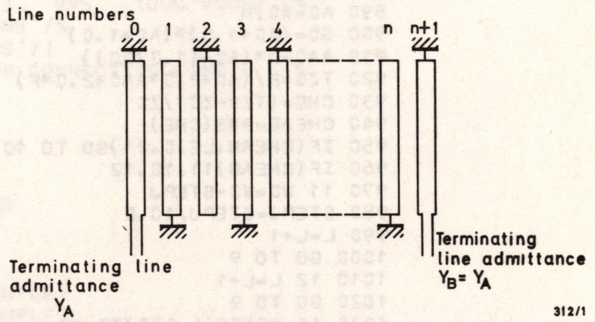
Line numbers
0
1
2
3
4
n
n+1
Terminating line admittance Y_A
Terminating line admittance $Y_B = Y_A$
312/1

Fig. 1—Interdigital filter with teminating lines short-circuited

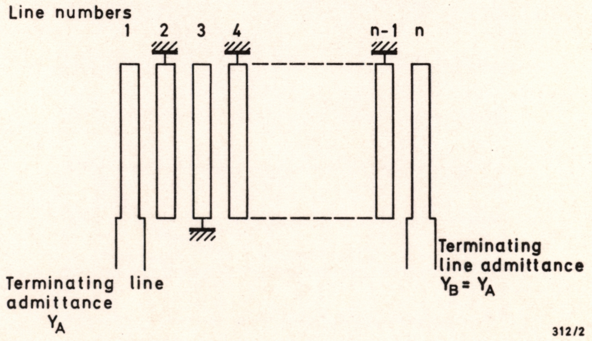
Line numbers
1
2
3
4
n-1
n
Terminating line admittance Y_A
Terminating line admittance $Y_B = Y_A$
312/2

Fig. 2—Interdigital filter with terminating lines open-circuited

The filter of Fig. 2 is different from that of Fig. 1 in that the terminating lines are open-circuited instead of short-circuited. This design is suitable for moderate to wide bandwidths (30% or greater relative to midband). In this case, all the line elements serve as resonators including the open-circuited terminating elements at each end.

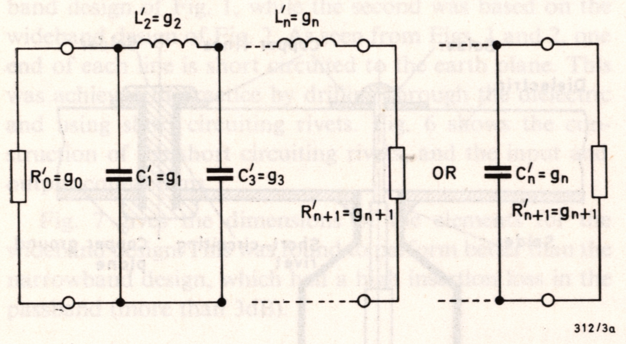

Fig. 3—Lowpass prototype defining filter parameters

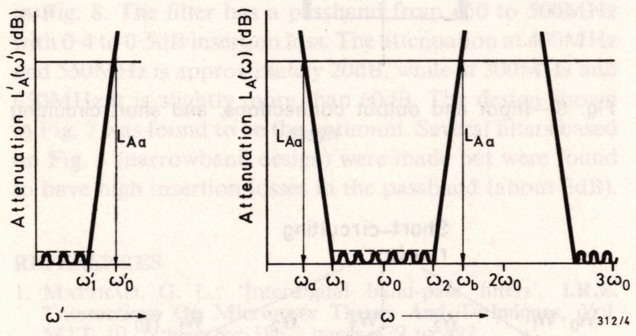

Fig. 4—Relationship between Chebychev response lowpass filter and required bandpass filter

Design values for the bandpass filter are derived from the lowpass prototype shown in Fig. 3. The filter parameters are as shown. Fig. 4 relates the Chebychev response of the lowpass filter to that of the required bandpass filter. The formulae for converting lowpass to bandpass are:

$$\mathrm{L_A}(\omega) = \mathrm{L'_A}(\omega'), \qquad \ldots(1)$$

and,

$$\omega_0 = \frac{\omega_2+\omega_1}{2}, \qquad \ldots(2)$$

where

$$\omega' = \frac{2\omega_1'}{\beta}\left|\frac{\omega-\omega_0}{\omega_0}\right|$$

and

$$\beta = \frac{\omega_2-\omega_1}{\omega_0}.$$

$\mathrm{L_A}(\omega)$ and $\mathrm{L'_A}(\omega')$ are values of attenuation in dB as functions of radial frequencies ω and ω', and β is the fractional bandwidth. The other radial frequencies are as defined in Fig. 4.

Values for prototype filters having Chebychev responses are given in Refs. 3, 4 and 5.

The transformation given in Eqs. 1 and 2 is only approximate and is usually considered to be useful only for filters of narrow or moderate bandwidth. However, it was found to work well with interdigital filters even in cases of quite large bandwidth (Ref. 1), provided that the parameter β is increased by about 7% to allow for approximations in the theory.

As mentioned earlier, interdigital filters consist of arrays of parallel line elements coupled to each other through their self and mutual capacitances. Design equations derived in Appendices 1 and 2 give the values of these capacitances per unit length. From these values, the actual dimensions of the lines can be determined. The various capacitances are defined by reference to Fig. 5 which shows an asymmetrical pair of parallel-coupled microstrip lines. C_a is the capacitance per unit length between line a and ground, C_{ab} is the capacitance between line a and line b, and C_b is the capacitance per unit length between line b and ground.

The odd and even mode capacitances for line a are:

$$C_{0o(a)} = C_a+2C_{ab}, \qquad C_{0e(a)} = C_a;$$

and for line b are:

$$C_{0o(b)} = C_b+2C_{ab}, \qquad C_{0e(b)} = C_b.$$

Having established the required values of the odd and even mode capacitances, the dimensions of the lines can be obtained. Getsinger (Ref. 6) has derived equations and charts for the various capacitances of coupled rectangular-bar lines, and Schwarzmann (Ref. 7) has derived similar equations for microstrip.

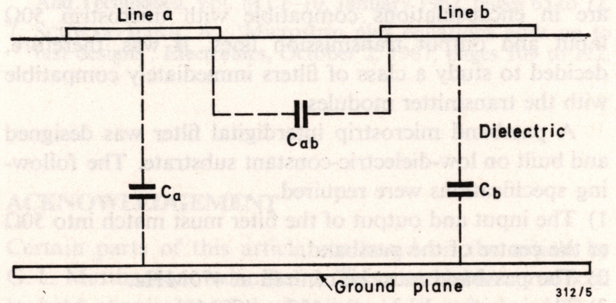

Fig. 5—Asymmetrical pair of parallel-coupled microstrip lines

Two sets of equations are derived in Appendices 1 and 2. One set (Appendix 1) is suitable for designing filters of narrow to moderate bandwidth of the structure shown in Fig. 1, and the other (Appendix 2) is suitable for filters of moderate to wide bandwidth of the structure shown in Fig. 2. In both cases, the mapping of Fig. 4 is used to select a low-pass prototype with the required number of elements. The element parameters (g_0, g_1, g_2 etc.) are then derived from the appropriate design equations, and the self capacitances and mutual capacitances are calculated.

The parameter h used in both sets of equations is a dimensionless admittance scale factor arbitrarily specified to give a convenient admittance level in the filter. One of the prime considerations in the choice of h is that the line dimensions must be such that the resonators will have a high unloaded Q. The dimensions giving optimum values of Q for resonator structures such as interdigital filters are not known. However, it is known that for air-filled, coaxial-line resonators the optimum Q will result when the line impedance is about 76Ω, and various approximate studies suggest that the optimum impedance for strip-line resonators is not greatly different. Matthaei (Ref. 1) suggests that for stripline filters, h is chosen so that, assuming an air dielectric,

$$\frac{2C_{k-1,\,k}}{\varepsilon_r}+\frac{C_k}{\varepsilon_r}+\frac{2C_{k,k+1}}{\varepsilon_r}\simeq 5{\cdot}4,$$

where $k = n/2$ for even n and $k = \frac{n+1}{2}$ for odd n.

$C_{k,\,k+1}$ is the mutual capacitance per unit length between line k and line k+1, and $C_{k,\,k-1}$ is the mutual capacitance between line k and line k−1, and C_k is the self capacitance per unit length of line k. For $\varepsilon_r=1$, the value of 5·4 for the above equation corresponds to making the line impedance of the resonator elements at the filter centre equal to 70Ω.

DESIGN EXAMPLE AT 470MHz

Specifications and construction

Mullard manufacture many components for radio telephone equipment as well as a range of modular wideband power amplifiers for the u.h.f. bands (380 to 512MHz). Circuit modules simplify the job of the circuit designer but shift the emphasis to obtaining the necessary frequency selectivity in a practical transmitter in which the spurious radiated emission must be less than 2·5μW at any frequency.

Normally a block bandpass filter will precede the modular amplifier, and a bandpass or lowpass filter will act as aerial filter. Furthermore, the modular amplifiers are in encapsulations compatible with microstrip 50Ω input and output transmission lines. It was, therefore, decided to study a class of filters immediately compatible with the transmitter modules.

A passband microstrip interdigital filter was designed and built on low-dielectric-constant substrate. The following specifications were required.

1) The input and output of the filter must match into 50Ω at the centre of the passband.

2) The passband must be centred at 470MHz.

3) The insertion loss in the 450 to 490MHz passband must not exceed 0·5dB.

4) Attenuation at 300MHz and at 650MHz must preferably be greater than 50dB.

A Chebychev response was chosen since it offers greater rates of attenuation in the stop bands than the equivalent Butterworth response. The above requirements can be met by a 3-section Chebychev filter with a 0·5dB ripple in the passband, but it was decided that a 7-section filter with a 0·01dB ripple in the passband and an attenuation of more than 70dB at 300 and 650MHz would be designed to compensate for inaccuracies in manufacture. This would ensure that the final product has a ripple of better than 0·5dB in the passband, and an attenuation of more than 50dB at 300MHz and 650MHz.

The first task was to establish the value of the parameter h to yield optimum line dimensions. As explained, h is chosen so that the resonators in the middle of the filter have a high Q, as condition that corresponds to a line impedance of about 75Ω. Computational methods using the theory given in Ref. 7 yielded a value for h of 0·073 for optimum performance. The values of the self and mutual capacitances C_k and $C_{k,\,k+1}$ per unit length were then calculated (Ref. 1). Schwarzman (Ref. 7) gives the self and mutual capacitances of coupled microstrip lines in terms of the relative dielectric contsant ε_r, the spacings between the lines, s, the ratio of line width to substrate thickness, W/H, and the ratio of line thickness to substrate thickness, t/H. Each capacitance is split into a number of components (the parallel plate capacitance and the various fringing capacitances) which can be calculated separately.

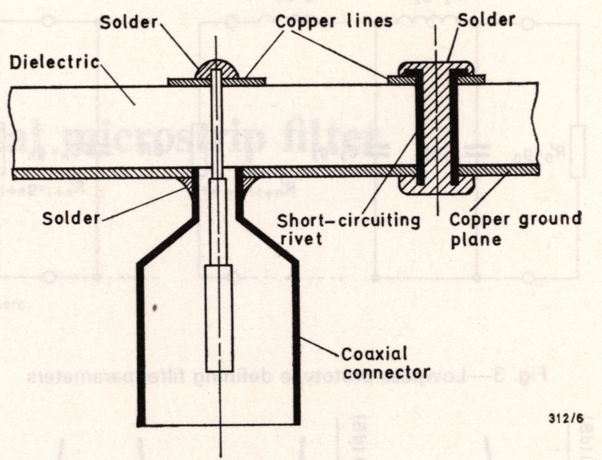

Fig. 6—Input and output connections, and short-circuiting rivets

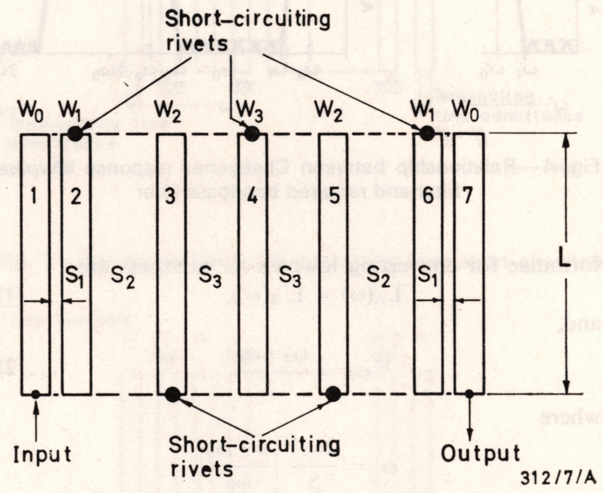

W_0 = 2·54mm
W_1 = 2·54mm
W_2 = 3·80mm
W_3 = 3·80mm
S_1 = 0·2mm
S_2 = 2·54mm
S_3 = 2·54mm
L = 107mm

Fig. 7—Bandpass filter element dimensions and spacings

The original specifications for the bandpass filter resulted in unpractical dimensions. In particular, the spacing between line 1 and line 2, and line 6 and line 7 was computed as 0·0762mm. Attempts to produce these dimensions accurately were not very successful. As a result of this, the specifications were relaxed.

Two filters were designed and built on Rexolite 1422 (ε_r=2·55, thickness of dielectric = $\frac{1}{16}$″, thickness of copper conductor = 0·0015″). The first was based on the narrowband design of Fig. 1, while the second was based on the wideband design of Fig. 2. As seen from Figs. 1 and 2, one end of each line is short circuited to the earth plane. This was achieved in practice by drilling through the dielectric and using short circuiting rivets. Fig. 6 shows the construction of the short circuiting rivets, and the input and output connections.

Fig. 7 gives the dimensions of the elements for the wideband design. This was found to perform better than the narrowband design, which had a high insertion loss in the passband (more than 3dB).

Performance of the filter

The performance of the wideband filter of Fig. 7 is shown in Fig. 8. The filter has a passband from 450 to 500MHz with 0·4 to 0·5dB insertion loss. The attenuation at 400MHz and 550MHz is approximately 20dB, while at 300MHz and 650MHz it is slightly more than 60dB. The design shown in Fig. 7 was found to be the optimum. Several filters based on Fig. 1 (narrowband design) were made but were found to have high insertion losses in the passband (about 3dB).

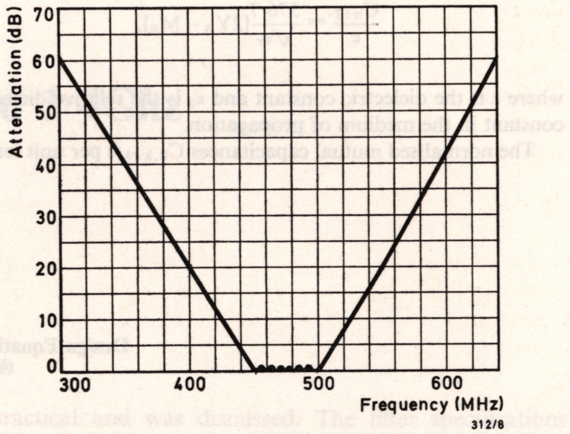

Fig. 8—Attenuation characteristic of filter in Fig. 7

REFERENCES

1. MATTHAEI, G. L., 'Interdigital band-pass filters', **I.R.E. Transactions On Microwave Theory and Techniques,** Vol. MTT–10, November 1962, pages 479 to 497.
2. MATTHAEI, G. L., 'Design of wide band (and narrow band) band-pass microwave filters on the insertion loss basis', **I.R.E. Transactions On Microwave Theory And Techniques,** Vol. MTT–8, November 1960, pages 580 to 593.
3. WEINBERG, L., 'Additional tables for design of optimum ladder networks', **J. Franklin Inst.,** Vol. 264, July and August 1957, pages 7 to 23 and 127 to 138.
4. MATTHAEI, G. L., *et al*, 'Design criteria for microwave filters and coupling structures', Standford Research Inst., Menlo Park Calif., Final Report SRI Project 2326 Contract DA36–039 SC–74862, January 1961.
5. ZVEREV, A. I., 'Handbook Of Filter Synthesis', John Wiley and Sons Inc., 1967, pages 310 to 340.
6. GETSINGER, W. J., 'Coupled rectangular bars between parallel plates', **I.R.E. Transactions On Microwave Theory And Techniques,** Vol. MTT–10, January 1962, pages 65 to 72.
7. SCHWARZMANN, A., 'Microstrip plus equations adds up to fast designs', **Electronics,** October 2, 1967, pages 109 to 112.

ACKNOWLEDGEMENT

Certain parts of this article are based on the article by G. L. Matthaei quoted in Ref. 1. This material is reproduced by kind permission of the Institute of Electrical and Electronics Engineers.

APPENDIX 1

Design Equations for Interdigital Filters of the Form in Fig. 1

Use mapping in Fig. 4 to select a low-pass prototype with the required value of n. The input and output lines in this filter do not count as resonators, so that there are n+2 lines for an n-reactive-element prototype.

Compute

$$\theta_1=\frac{\pi}{2}\,\frac{\omega_1}{\omega_0}=\frac{\pi}{2}\left(1-\frac{\beta}{2}\right)$$

$$\frac{J_{01}}{Y_A}=\frac{1}{\sqrt{g_0g_1\omega_1'}},\quad \left.\frac{J_{k,k+1}}{Y_A}\right|_{k=1\text{ to }n-1}=\frac{1}{\omega_1'\sqrt{g_kg_{k+1}}}$$

$$\frac{J_{n,n+1}}{Y_A}=\frac{1}{\sqrt{g_ng_{n+1}\omega_1'}},$$

$$\left.N_{k,k+1}\right|_{k=1\text{ to }n-1}=\sqrt{\left(\frac{J_{k,k+1}}{Y_A}\right)^2+\frac{\tan^2\theta_1}{4}}$$

$$M_1=Y_A\left[\frac{J_{01}}{Y_A}\sqrt{h}+1\right],\qquad M_n=Y_A\left[\frac{J_{n,n+1}}{Y_A}\sqrt{h}+1\right]$$

where h is a dimensionless admittance scale factor to be specified arbitrarily so as to give a convenient admittance level in the filter. (See text.)

The normalised self-capacitances C_k/ε per unit length for the line elements are:

$$\frac{C_0}{\varepsilon}=\frac{376{\cdot}7}{\sqrt{\varepsilon_r}}[2Y_A-M_1]$$

$$\frac{C_1}{\varepsilon}=\frac{376{\cdot}7}{\sqrt{\varepsilon_r}}\left[Y_A-M_1+hY_A\left(\frac{\tan\theta_1}{2}+\left(\frac{J_{01}}{Y_A}\right)^2+N_{12}-\frac{J_{12}}{Y_A}\right)\right]$$

$$\left.\frac{C_k}{\varepsilon}\right|_{k=2\text{ to }n-1}=\frac{376{\cdot}7}{\sqrt{\varepsilon_r}}hY_A\left[N_{k-1,k}+N_{k,k+1}-\frac{J_{k-1,k}}{Y_A}-\frac{J_{k,k+1}}{Y_A}\right]$$

$$\frac{C_n}{\varepsilon}=\frac{376{\cdot}7}{\sqrt{\varepsilon_r}}\left[Y_A-M_n+hY_A\times\right.$$

$$\left.\times\left(\frac{\tan\theta_1}{2}+\left(\frac{J_{n,n+1}}{Y_A}\right)^2+N_{n-1,n}-\frac{J_{n-1,n}}{Y_A}\right)\right]$$

$$\frac{C_{n+1}}{\varepsilon} = \frac{376{\cdot}7}{\sqrt{\varepsilon_r}}[2Y_A - M_n],$$

where ε is the dielectric constant and ε_r is the relative dielectric constant in the medium of propagation.

The normalised mutual capacitances $C_{k,k+1}/\varepsilon$ per unit length between adjacent line elements are

$$\frac{C_{01}}{\varepsilon} = \frac{376{\cdot}7}{\sqrt{\varepsilon_r}}[M_1 - Y_A],$$

$$\left.\frac{C_{k,k+1}}{\varepsilon}\right|_{k=1 \text{ to } n-1} = \frac{376{\cdot}7hY_A}{\sqrt{\varepsilon_r}}\left(\frac{J_{k,k+1}}{Y_A}\right),$$

$$\frac{C_{n,n+1}}{\varepsilon} = \frac{376{\cdot}7}{\sqrt{\varepsilon_r}}[M_n - Y_A].$$

APPENDIX 2

Design Equations for Interdigital Filters of the Form in Fig. 2

Use mapping in Fig. 4 to select low-pass prototype with the required value of n. The input and output lines in this filter count as resonators, so that there are n line elements for an n-reactive-element prototype. Compute

$$\theta_1 = \frac{\pi}{2}\frac{\omega_1}{\omega_0} = \frac{\pi}{2}\left(1 - \frac{\beta}{2}\right)$$

$$\left.\frac{J_{k,k+1}}{Y_A}\right|_{k=2 \text{ to } n-3} = \frac{g_2}{g_0\sqrt{g_k g_{k+1}}}, \quad \frac{J_{n-2,n-1}}{Y_A} = \frac{1}{g_0}\sqrt{\frac{g_0 g_2}{g_{n-2}g_{n+1}}}$$

$$\left.N_{k,k+1}\right|_{k=2 \text{ to } n-2} = \sqrt{\left[\left(\frac{J_{k,k+1}}{Y_A}\right)^2 + \left(\frac{\omega_1' g_2 \tan\theta_1}{2g_0}\right)^2\right]}$$

$$\frac{Z_1}{Z_A} = \omega_1' g_0 g_1 \tan\theta_1$$

$$\frac{Y_2}{Y_A} = \frac{\omega_1' g_2}{2g_0}\tan\theta_1 + N_{23} - \frac{J_{23}}{Y_A}$$

$$\left.\frac{Y_k}{Y_A}\right|_{k=3 \text{ to } n-2} = N_{k-1,k} + N_{k,k+1} - \frac{J_{k-1,k}}{Y_A} - \frac{J_{k,k+1}}{Y_A}$$

$$\frac{Y_{n-1}}{Y_A} = \frac{\omega_1'(2g_0 g_{n-1} - g_2 g_{n+1})\tan\theta_1}{2g_0 g_{n+1}} + N_{n-2,n-1} - \frac{J_{n-2,n-1}}{Y_A}$$

$$\frac{Z_n}{Z_A} = \omega_1' g_n g_{n+1} \tan\theta_1.$$

The normalised self-capacitances, C_k/ε, per unit length for the line elements are

$$\frac{C_1}{\varepsilon} = \frac{367{\cdot}7}{\sqrt{\varepsilon_r}}Y_A\frac{(1-\sqrt{h})}{(Z_1/Z_A)}$$

$$\frac{C_2}{\varepsilon} = \frac{376{\cdot}7}{\sqrt{\varepsilon_r}}Y_A h\left(\frac{Y_2}{Y_A}\right) - \sqrt{h}\frac{C_1}{\varepsilon}$$

$$\left.\frac{C_k}{\varepsilon}\right|_{k=3 \text{ to } n-2} = \frac{376{\cdot}7}{\sqrt{\varepsilon_r}}Y_A h\left(\frac{Y_k}{Y_A}\right)$$

$$\frac{C_{n-1}}{\varepsilon} = \frac{376{\cdot}7}{\sqrt{\varepsilon_r}}Y_A h\left(\frac{Y_{n-1}}{Y_A}\right) - \sqrt{h}\frac{C_n}{\varepsilon}$$

$$\frac{C_n}{\varepsilon} = \frac{376{\cdot}7}{\sqrt{\varepsilon_r}}Y_A\frac{(1-\sqrt{h})}{(Z_n/Z_A)}$$

where ε is the dielectric constant, ε_r is the relative dielectric constant in the medium of propagation, and h is a dimensionless admittance scale factor whose value should be chosen to give a convenient admittance level in the filter. (See text.)

The normalised mutual capacitances $C_{k,k+1}/\varepsilon$ per unit length between adjacent line elements are

$$\frac{C_{12}}{\varepsilon} = \frac{376{\cdot}7}{\sqrt{\varepsilon_r}}Y_A\frac{\sqrt{h}}{(Z_1/Z_A)}$$

$$\left.\frac{C_{k,k+1}}{\varepsilon}\right|_{k=2 \text{ to } n-2} = \frac{376{\cdot}7}{\sqrt{\varepsilon_r}}Y_A h\left(\frac{J_{k,k+1}}{Y_A}\right)$$

$$\frac{C_{n-1,n}}{\varepsilon} = \frac{376{\cdot}7}{\sqrt{\varepsilon_r}}Y_A\frac{\sqrt{h}}{(Z_n/Z_A)}.$$

Microstrip bandpass filter for 0·7 to 1·4Ghz

The design and construction of a Chebychev microstrip bandpass filter consisting of a number of λ/4 short circuited stubs spaced by λ/4 lines is described. Two versions of the filter are given. The first has an insertion loss of less than 1dB from 700MHz to 1350MHz and an attenuation of 25dB at 470MHz and 1570MHz. The second has an insertion loss of less than 1dB from 700MHz to 1450MHz, and an attenuation of 25dB at 470MHz and 1700MHz.

INTRODUCTION

A standard computer program, developed at the Mullard Research Laboratories, can be used to design microstrip bandpass filters each consisting of a number of λ/4 short-circuited stubs spaced by lines, λ/4 in length. The filters are designed to have Chebychev equal-ripple characteristics. Given the required filter specifications and microstrip board data, including the minimum acceptable line width, the program computes the dimensions of the filter and performs a test. It then either passes the design, or modifies the dimensions to improve it.

Filters were required for measuring second harmonics in the BGY22 and BGY23 u.h.f. modules. These modules operate in the frequency range 380 to 512MHz, and therefore, for second harmonic measurements, filters are required which have high insertion losses in this range but which pass frequencies in the range 760 to 1024MHz.

FILTER SPECIFICATIONS AND COMPUTED RESULTS

The design filter consists of a number of λ/4 short-circuited stubs spaced by λ/4 lines. The original specifications were as follows:

Passband	0·6 to 2·0GHz
V.S.W.R. in the passband	1·2 max
Impedance	50Ω
Attenuation	30dB at 0·47GHz
Microstrip board	Permaflon
Minimum acceptable line width	0·127mm (0·005″)
Thickness of copper conductor	0·0762mm (0·003″, 2oz Cu)
Thickness of dielectric	1·5875mm ($\frac{1}{16}$″)
Relative dielectric constant	2·74

With these specifications the computer program gave a 14-node filter, symmetrical about the centre, with stub widths varying from 0·2mm to 0·5mm. The total length of the filter was about 600mm. This design was considered unpractical and was dismissed. The filter specifications were then relaxed to the following:

Passband	0·7 to 1·4GHz
V.S.W.R. in the passband	1·2 max
Impedance	50Ω
Attenuation	20dB at 0·47GHz
Microstrip board	Permaflon
Minimum acceptable line width	0·127mm (0·005″)
Thickness of copper conductor	0·0762mm (0·003″, 2oz Cu)
Thickness of dielectric	1·5875mm ($\frac{1}{16}$″)
Relative dielectric constant	2·74

The computer program gave a 6-node filter, symmetrical about the centre. The computed results for one half of the symmetrical filter are given in Tables 1, 2 and 3.

TABLE 1

Computed admittances and impedances

Node	Stub admittance (mho)	Line admittance (mho)	Stub impedance (Ω)	Line impedance (Ω)
1	0·01560		64·101	
		0·02336		42·802
2	0·03105		32·206	
		0·02374		42·118
3	0·03135		31·898	
		0·02263		44·197

TABLE 2

Computed v.s.w.r. and insertion loss

Frequency (GHz)	V.S.W.R.	Insertion loss (dB)
0·47	1540·5	25·862
0·7	1·2000	0·03604

TABLE 3

Computed filter dimensions

Node	Width (stub) (mm)	Width (line) (mm)	Number of stubs	Length (stub) (mm)	Length (line) (mm)
0	0·0000		0	0·0000	
		4·1830			47·6951
1	2·7841		1	48·3583	
		5·2827			47·3110
2	2·7607		2	48·3719	
		5·4079			47·2723
3	2·8073		2	48·3449	
		5·0399			47·3886

CONSTRUCTION OF FILTER

A schematic diagram of a 6-node filter is shown in Fig. 1. The filter proper starts at stub S(1). Line L(0) is the feed line, length λ/4 and width corresponding to 50Ω. This line has no great effect on the performance.

In the computed design, stubs S(1) are 64Ω impedance single stubs, while the others are double stubs, each 64Ω, which in parallel give the desired 32Ω impedance. The filter is shown diagrammatically in Fig. 2.

Two versions of the design are shown in Figs. 3 and 4. The first (Fig. 3) comprises 10 stubs (2 singles and 4 doubles), each connected to a λ/4 low-impedance line which is left open-circuited at the other end. In this way, the open circuit is transformed to a short circuit at the stub. The advantage of this method is that the line and earth plane are d.c. isolated from each other. In the second version of the filter (Fig. 4), all the stubs are short-circuited to the earth plane through rivets.

The input and output connections to both filters, and the short circuiting rivets, are as shown in Fig. 5.

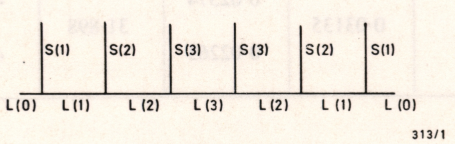
S(1)
S(2)
S(3)
S(3)
S(2)
S(1)
L(0)
L(1)
L(2)
L(3)
L(2)
L(1)
L(0)
313/1

Fig. 1—Schematic diagram of 6-node symmetrical filter

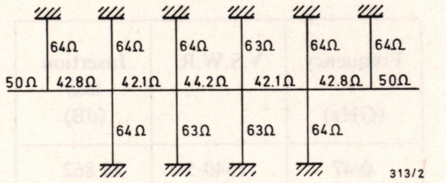
64Ω
64Ω
64Ω
63Ω
64Ω
64Ω
50Ω
42.8Ω
42.1Ω
44.2Ω
42.1Ω
42.8Ω
50Ω
64Ω
63Ω
63Ω
64Ω
313/2

Fig. 2—Computed 6-node symmetrical filter

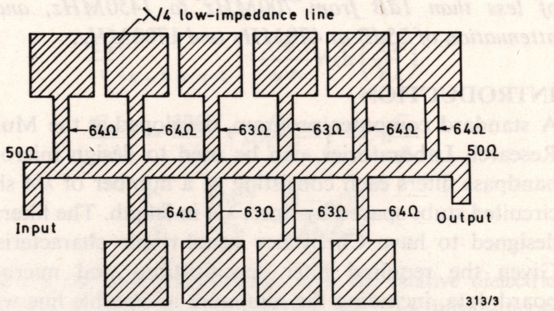
λ/4 low-impedance line
50Ω
64Ω
64Ω
63Ω
63Ω
64Ω
64Ω
50Ω
Input
64Ω
63Ω
63Ω
64Ω
Output
313/3

Fig. 3—Microstrip filter with λ/4 stubs connected to λ/4 low-impedance lines

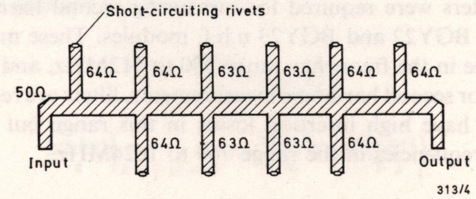
Short-circuiting rivets
50Ω
64Ω
64Ω
63Ω
63Ω
64Ω
64Ω
50Ω
64Ω
63Ω
63Ω
64Ω
Input
Output
313/4

Fig. 4—Microstrip filter with stubs short-circuited

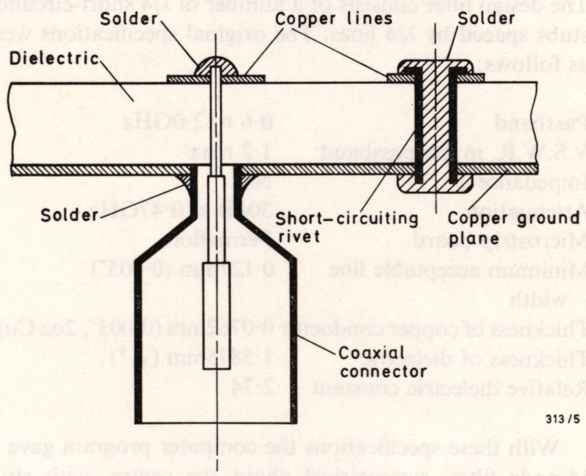
Solder
Copper lines
Solder
Dielectric
Solder
Short-circuiting rivet
Copper ground plane
Coaxial connector
313/5

Fig. 5—Input and output connections and short-circuiting rivets

EXPERIMENTAL RESULTS

The properties of both filters were measured on a Hewlett Packard Microwave Network Analyser. Figs. 6 to 8 give the performance of the filter of Fig. 3, while Figs. 9 to 11 give the performance of the filter of Fig. 4.

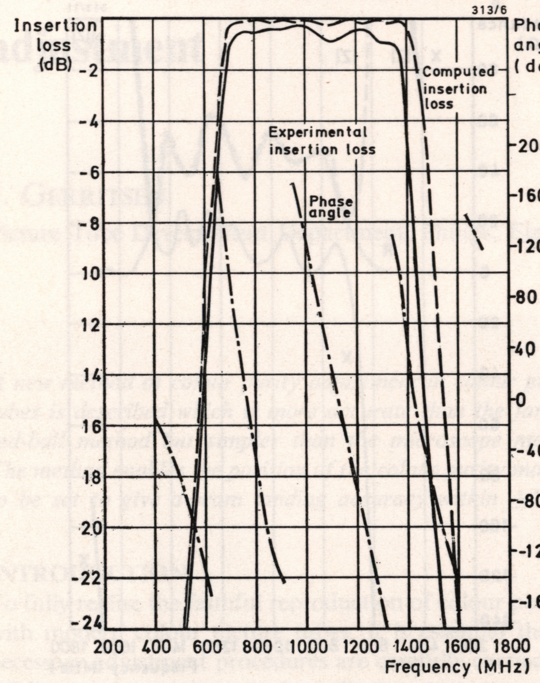

Fig. 6—Insertion loss and phase angle between input and output plotted against frequency for the filter of Fig. 3

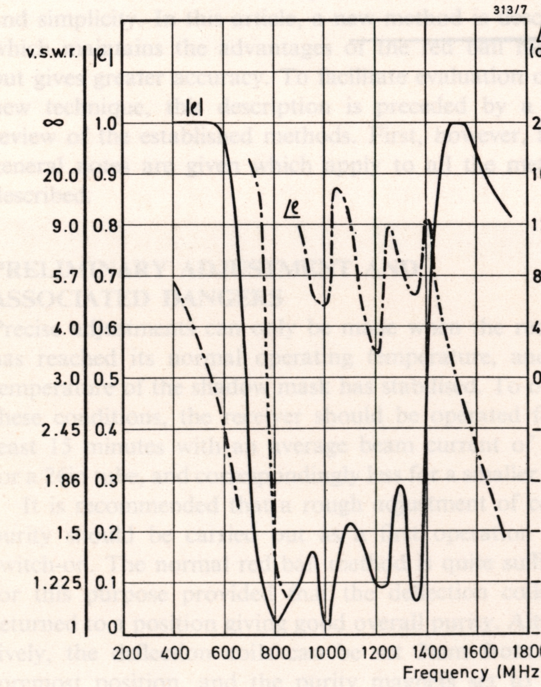

Fig. 7—Magnitude and angle of input reflection coefficient plotted against frequency for the filter of Fig. 3

Fig. 6 shows the insertion loss and the relative phase angle between input and output as functions of frequency for the filter of Fig. 3. The computed insertion loss is also included for comparison. The two curves are in good agreement, although the experimental passband is about

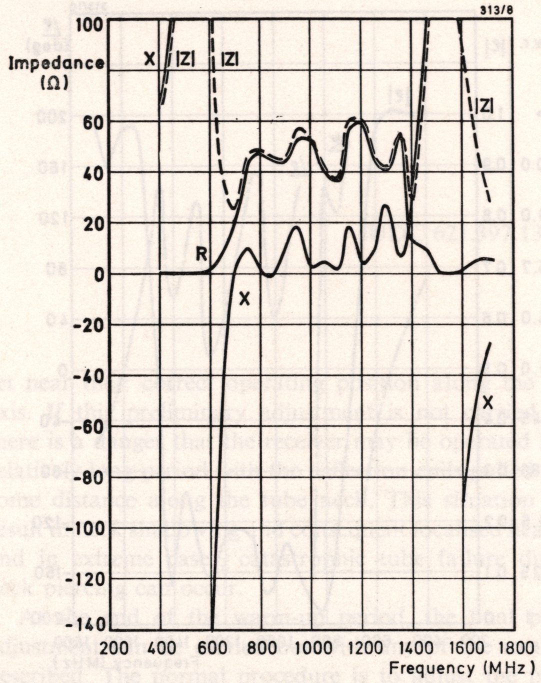

Fig. 8—Input impedance (Z = R + jX) plotted against frequency for the filter of Fig. 3

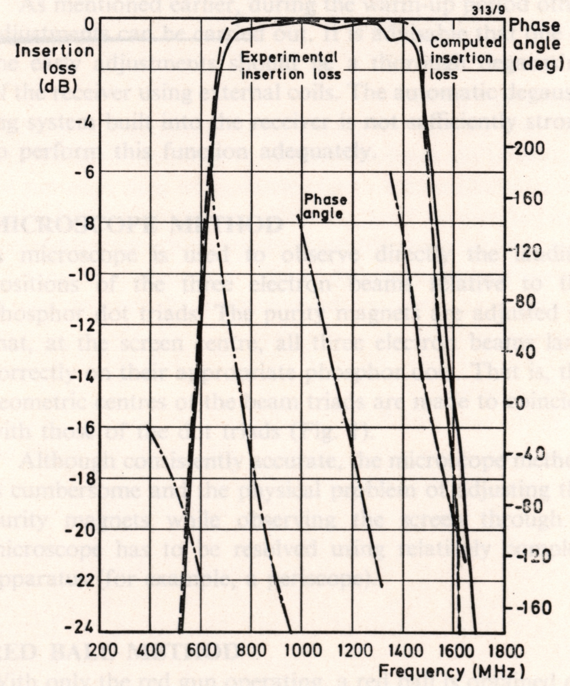

Fig. 9—Insertion loss and phase angle between input and output plotted against frequency for the filter of Fig. 4

10% less than the theoretical value, and the insertion loss in the passband of the experimental filter is greater. The magnitude and phase angle of the reflection coefficient plotted against frequency are shown in Fig. 7. A v.s.w.r. scale is also given. Fig. 8 shows the resistive and reactive parts, and the modulus, of the input impedance of the filter.

Figs. 9 to 11 give the equivalent information for the filter of Fig. 4. It can be seen from Fig. 9 that, when compared with the filter of Fig. 3, there is closer agreement between the computed and experimental curves for insertion loss against frequency.

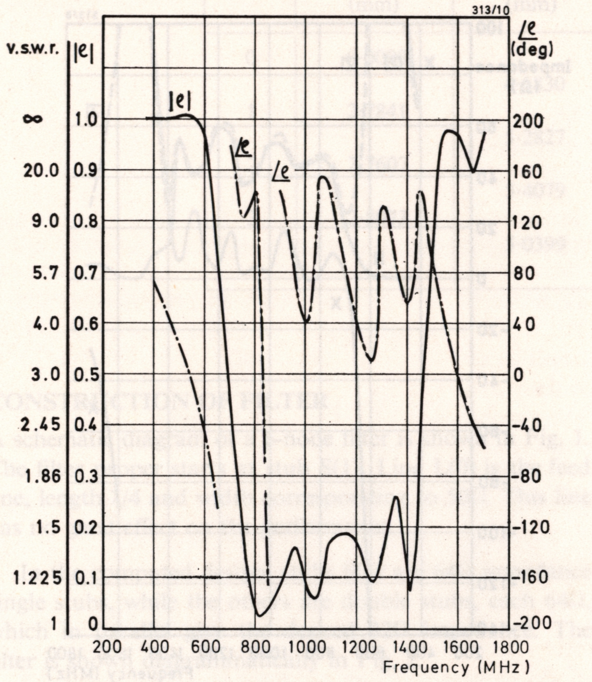

Fig. 10—Magnitude and angle of input reflection coefficient plotted against frequency for the filter of Fig. 4

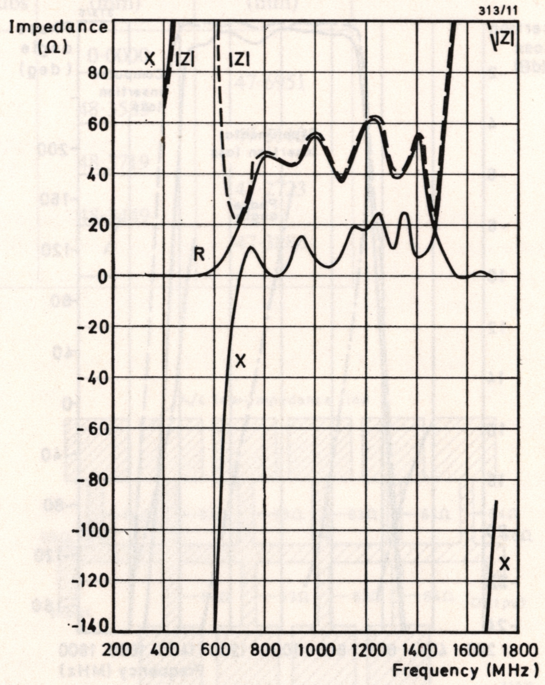

Fig. 11—Input impedance (Z = R + jX) plotted against frequency for the filter of Fig 4

A new method of colour purity adjustment

J. GERRITSEN
Picture Tube Development Department, Philips, Eindhoven.

UDC 621.397.132–53

A new method of colour purity adjustment in colour picture tubes is described which is more accurate than the familiar red-ball method but simpler than the microscope method. The method enables the position of the colour purity magnets to be set to give a beam landing accuracy within ±10μm.

INTRODUCTION

To fully realise the faithful reproduction of colour possible with modern colour picture tubes, it is essential that all necessary adjustment procedures are carefully carried out. With regard to colour purity adjustment, two methods are at present in use: the 'microscope' method and the 'red ball' method. Although the superiority of the microscope method in terms of accuracy is indisputable, the red ball method is more widely used because of its speed and simplicity. In this article, a new method is described which maintains the advantages of the red ball method but gives greater accuracy. To facilitate evaluation of the new technique, this description is preceded by a brief review of the established methods. First, however, a few general notes are given which apply to all the methods described.

PRELIMINARY ADJUSTMENT AND ASSOCIATED DANGERS

Precise adjustments can only be made when the receiver has reached its normal operating temperature, and the temperature of the shadow mask has stabilised. To obtain these conditions, the receiver should be operated for at least 15 minutes with an average beam current of 1mA for a 26in tube, and correspondingly less for a smaller tube.

It is recommended that a rough adjustment of colour purity should be carried out as a first operation after switch-on. The normal red ball method is quite sufficient for this purpose provided that the deflection coils are returned to a position giving good overall purity. Alternatively, the deflection coils can be set 3mm from their foremost position, and the purity magnets set to zero. Both approaches not only allow other adjustments to be carried out while the receiver is warming up but, what is more important, also ensure that the deflection coils are set near their correct operating position along the tube axis. If this preliminary adjustment is not carried out, there is a danger that the receiver may be operated for a relatively long period with the deflection coils pulled back some distance along the tube neck. This situation may result in neck shadowing and consequent localised heating, and in extreme cases, catastrophic tube failure due to neck piercing can occur.

At the end of the warm-up period, the final purity adjustment can be carried out with any of the methods described. The normal procedure is to adjust the purity at the centre of the screen by means of the purity magnets, and then to obtain a pure raster over the whole screen by careful positioning of the deflection coils along the tube axis.

As mentioned earlier, during the warm-up period other adjustments can be carried out. It is advisable that one of the early adjustments should be a thorough degaussing of the receiver using external coils. The automatic degaussing system built into the receiver is not sufficiently strong to perform this function adequately.

MICROSCOPE METHOD

A microscope is used to observe directly the landing positions of the three electron beams relative to the phosphor dot triads. The purity magnets are adjusted so that, at the screen centre, all three electron beams land correctly on their appropriate phosphor dots. That is, the geometric centres of the beam triads are made to coincide with those of the dot triads (Fig. 1).

Although consistently accurate, the microscope method is cumbersome and the physical problem of adjusting the purity magnets while observing the screen through a microscope has to be resolved using relatively complex apparatus (for example, a periscope).

RED BALL METHOD

With only the red gun operating, a red ball is obtained on the screen by pulling back the scan coil assembly as far as it will go along the neck of the tube. The purity magnets are then adjusted so that the centre of the red ball is

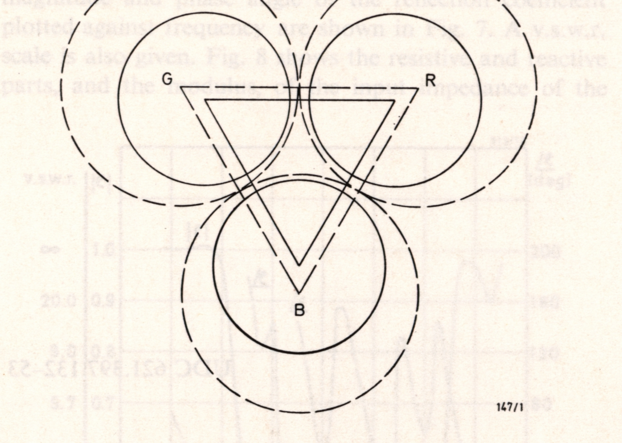

Fig. 1—Correct beam landing

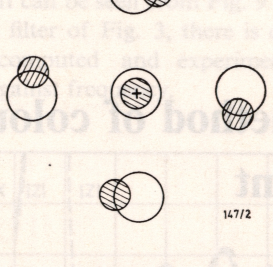

Fig. 2—Rotation of beam landing in new method

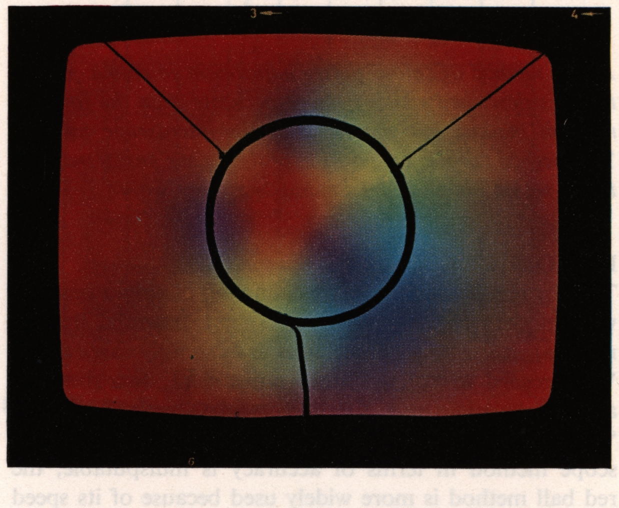

Fig. 3—The effect of the coil on a red raster. The red area is not centred in the coil, indicating misadjustment of the purity magnets

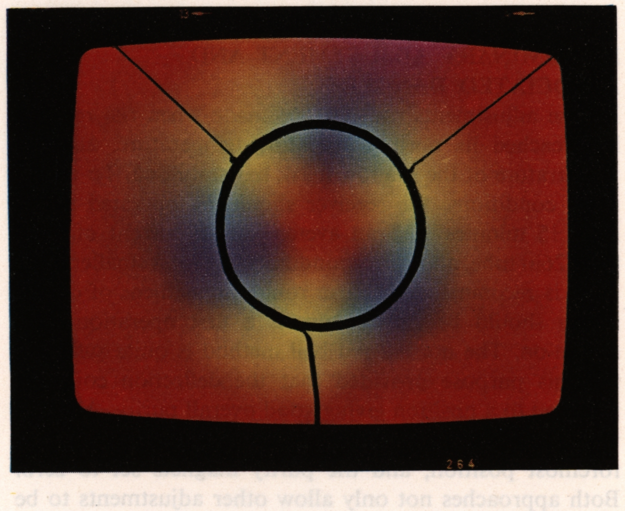

Fig. 4—The effect of the coil on a red raster with the purity magnets correctly adjusted. The red area is centred in the coil

situated approximately 20mm in the 8 o'clock direction from the screen centre; that is, in the direction of the red gun. After the purity magnets have been adjusted, the scan coil assembly is restored to its correct axial position and finally adjusted to give a pure red raster over the whole screen.

Although popular with set makers because of its simplicity, the red ball method has serious drawbacks. In contrast to the microscope method, purity adjustment is carried out with the deflection coils pulled back from the colour deflection centres. This introduces a systematic error which increases in proportion to the magnitude of purity correction. Although this error is generally small for the majority of tubes, in some cases it can reach significant proportions.

NEW METHOD

The new method* of colour purity adjustment is a modification of the red ball method. In this case, however, the red ball is formed not by retracting the scan coils but by external means. Thus, as with the microscope technique, the scan coil assembly can be left in the position selected during the preliminary rough adjustment of purity. Furthermore, because the formation of the red ball is obtained with the scan coils more or less in their optimum position, the new method is not subject to a built-in adjustment error.

In the new method, the red ball is obtained by placing a specially made coil in front of the screen on which an unmodulated red raster is displayed. The coil is thin and circular and is placed in contact with the tube face, its axis coincident with the tube axis. When a direct current is passed through the coil, the resulting field rotates the beam landing (Fig. 2) and a clearly defined red ball appears. The position of the ball depends on the adjustment of the colour purity magnets. The effect of the coil on a red raster is shown in Fig. 3 and 4. In Fig. 3, the red ball is not centred, indicating misadjustment of the purity magnets. In Fig. 4, the purity magnets are correctly adjusted.

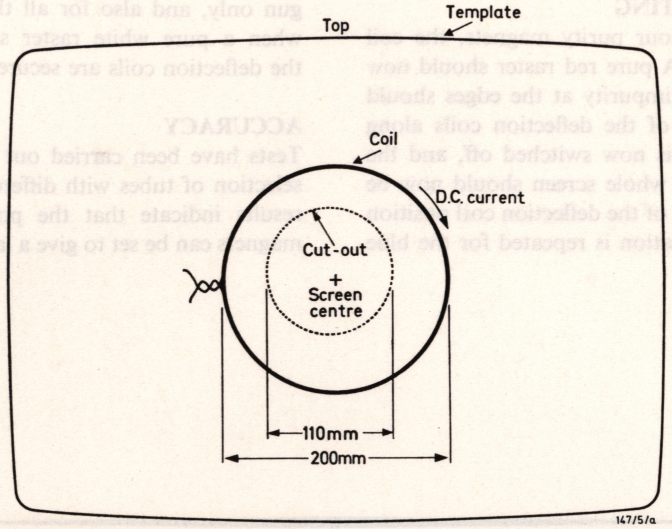

Fig. 5—Template, cut-out and coil arrangement used in new method

An opaque template (Fig. 5) is used to centre the coil precisely on the screen. The circular guide hole cut in the template helps when positioning the red ball. For tubes without centre beam landing precompression, the red ball should be coaxial with the tube axis. Hence, the template guide hole is positioned in the centre of the template. For tubes with centre beam landing precompression, however, it is necessary to set the red ball slightly off-centre (as in the old red ball method). If the coil current flows clockwise, the off-centre displacement will be towards 11 o'clock; conversely, if the current flows anti-clockwise, the displacement will be towards 5 o'clock. In both cases, the required off-centre displacement is one sixth of the red ball diameter. Therefore, to make adjustment easier with tubes of this type, the circular cut-out in the template should be off-centred accordingly, as shown in Fig. 5 (dotted). (Note that the coil remains central.)

The advantages of the method are:

1) Adjustment of the purity magnets is quickly and easily accomplished at the rear of the set while observing the screen in a mirror (aligned with the tube axis to eliminate parallax errors due to the thickness of the screen glass).
2) The only apparatus required is a coil, template, and d.c. supply.
3) Adjustment accuracy is comparable with that obtained using the microscope method.

Practical details

A coil 200mm in diameter, consisting of 80 turns of 0·5mm diameter wire, has been found to produce the best results.

The diameter of the red ball depends on the magnitude of the coil current. If the diameter is too large (small coil current), it becomes blurred and more difficult to adjust; if it is too small, the setting accuracy at the coil's centre decreases. A ball diameter of 40 to 50mm gives the best results.

The template should be carefully constructed so that the coil is accurately centred on the screen. A 10mm error in coil centring will result in a 5μm purity magnet adjustment error for a 90° tube, and a 7μm error for a 110° tube.

The following example gives some idea of the magnitude of coil current required (coil diameter 200mm in close contact with screen glass).

Required m.m.f.	60 ampere-turns (90° tube); 80 ampere-turns (110° tube)
Red ball diameter	48mm
Adjustment sensitivity	3mm displacement per 10μm purity magnet correction

The template cut-out should be about 110mm in diameter and positioned 8mm off-centre, the displacement being towards 11 o'clock (current clockwise) or 5 o'clock (current anti-clockwise).

As previously stated, the apparatus can consist of just the coil, template and d.c. supply, but it may be advantageous to include a degaussing system. This will remove the residual magnetism in the shadow mask, caused by the externally applied field. Degaussing can easily be achieved, when adjustment is completed, by switching the coil over to an a.c. supply in series with one or more degaussing PTC thermistors. A degaussing time of about 10 seconds is sufficient. To avoid the possibility of superimposing a d.c. component on to the degaussing current, the switch-over should be break-before-make.

---

*Sometimes termed the 'mini red ball' method.

DEFLECTION COIL SETTING

After adjustment of the colour purity magnets, the coil and template are removed. A pure red raster should now be seen on the screen. Any impurity at the edges should be removed by adjustment of the deflection coils along the tube axis. The red gun is now switched off, and the green gun switched on. The whole screen should now be green but a slight adjustment of the deflection coil position may be necessary. This operation is repeated for the blue gun only, and also for all three guns operating together when a pure white raster should be observed. Finally, the deflection coils are secured.

ACCURACY

Tests have been carried out using the new method on a selection of tubes with different scan coil assemblies. The results indicate that the position of the colour purity magnets can be set to give a landing accuracy within 10μm.